

Title	光電導性非晶質高分子固体におけるキャリア輸送に関する研究
Author(s)	藤野, 正家
Citation	大阪大学, 1984, 博士論文
Version Type	VoR
URL	https://hdl.handle.net/11094/167
rights	
Note	

Osaka University Knowledge Archive : OUKA

<https://ir.library.osaka-u.ac.jp/>

Osaka University

**STUDIES ON CHARGE CARRIER TRANSPORT IN AMORPHOUS
PHOTOCONDUCTIVE POLYMERS**

（光電導性非晶質高分子固体における）
キャリア輸送に関する研究

MASAE FUJINO

**STUDIES ON CHARGE CARRIER TRANSPORT IN AMORPHOUS
PHOTOCONDUCTIVE POLYMERS**

（光電導性非晶質高分子固体における
キャリア輸送に関する研究）

MASAIE FUJINO

Preface

The study of this thesis was carried out under the guidance of Professor Hiroshi Mikawa at Faculty of Engineering, Osaka University.

The subject of this thesis is to investigate the charge carrier transport in amorphous photoconductive polymers and to give a guide for finding the more photosensitive organic materials as the photoreceptors in electrophotography. The author hopes that the knowledges obtained in this study would give useful informations in developing photosensitive devices.

A handwritten signature in cursive script that reads "Masaie Fujino". The signature is written in black ink and is centered on the page.

Masaie Fujino

Course of Chemical Process Engineering

Faculty of Engineering

Osaka University

Yamadaoka, Suita, Osaka

JAPAN

January, 1984

Contents

General Introduction	1
Chapter 1 Drift Mobility in Amorphous Photoconductive Polymers	6
1-1 Introduction	6
1-2 Experimental	7
1-3 T_0 in PVCz - <u>Low-molecular Weight</u> Model Compound Systems	10
1-4 T_0 and Segmental Motion	16
1-5 Relationship between T_0 and μ_0	19
1-6 Annealing Effect	21
1-7 Conclusion	26
Chapter 2 Trap-Free Drift Mobility in Amorphous Photoconductive Polymers	29
2-1 Introduction	29
2-2 Method of Analysis	31
2-3 Evaluation of μ_f and Field Dependence	34
2-4 Initial Peak Current	36
2-5 Temperature Dependence of μ_f	38
2-6 Microscopic Carrier Transport	42
2-7 Conclusion	45

Chapter 3 Control of Carrier Trap in Amorphous Photoconductive Polymers 46

3-1 Introduction 46

3-2 Drift Mobility in Low-molecular Weight Compound Doped PVCz System 47

3-3 Drift Mobility in PVCz-ClTPP Binary System 49

3-4 Two-Step Detrapping Mechanism 54

3-5 Estimation of Parameters in Eq. (3-12) 59

3-6 ClTPP Concentration Dependence of $\mu(m)/\mu(0)$ 61

3-7 Conclusion 65

Summary 66

References 69

List of Publications 73

Acknowledgement 74

General Introduction

Photoconductivity is one of the important properties of materials used in the practical functional devices such as photodetectors, photosensors, solar cells, photoreceptors in electrophotography and so on. The photoconduction in selenium was first discovered in 1873 by R. Smith [1] and in 1906 the photoconduction in an organic material was first reported in anthracene by A. Pochettio [2]. In 1959 H. Hoegl et al. [3] found that some of organic vinyl polymers having a large π -electron system as a pendant group show the large photoconductivity. At present, photoconduction phenomenon has been recognized in many inorganic as well as organic materials.

From the practical viewpoint, especially when a large photosensitive area is required as in photoreceptor or solar cell, amorphous photoconductive polymer is one of the attractive materials because of the facility of the film fabrication. A large number of studies on the photoconduction phenomenon in the amorphous photoconductive polymers have been made for the purpose of the better understanding of the practical use of these materials in electrophotographic system. Many studies have also been reported for the basic understanding of the phenomenon itself in these materials. A lot of studies have been done focusing on the charge carrier transport phenomena. A deeper understanding of the charge carrier transport process

in amorphous polymers will provide an advanced step to find more sensitive materials.

Experimentally, a time-of-flight technique in the pulse photoconduction measurements is widely used in order to study the carrier transport process in the materials. The transient photocurrent signal observed in amorphous polymers shows an initial spike followed by an apparent plateau region and a long tail after the transit time, showing a great contrast to that of an ideal case which can be often observed in molecular single crystals.

The drift mobility of the charge carrier obtained in amorphous polymers always shows the much smaller values of the order of $10^{-7} - 10^{-6} \text{ cm}^2/\text{sec.V}$ as compared with the values of about $1 \text{ cm}^2/\text{sec.V}$ in molecular single crystals such as anthracene. P.J. Regensburger [4] pointed out that the drift mobility in amorphous polymers shows the strong field and temperature dependences due to the field-assisted thermal hopping from trap to trap in a typical photoconductive polymer, i.e., poly-N-vinylcarbazole (PVCz) by xerographic technique. From the measurements of the drift mobility by time-of-flight technique in PVCz and PVCz-TNF (2,4,7-trinitrofluorenone) systems, W.D. Gill [5] proposed experimentally an empirical expression which well represents the field and temperature dependences of the drift mobility in amorphous polymers. This equation has since been accepted for a wide variety of amorphous photoconductive polymers.

Many attempts have been made to account for the transient process of the charge carrier in such amorphous materials [3-20]. Seki [21] introduced the energy fluctuation of the hopping sites for the thermally activated tunnel hopping conduction. Scher and Montroll [22] proposed Continuous Time Random Walk (CTRW) theory in which the concept of the time-distribution of hopping events was introduced to explain the transient photocurrent shape. Pfister [18] modified the CTRW theory to apply to organic photoconductive polymers. Marshall et al. [23] gave an alternative interpretation of the pulse photocurrent shape by thermally activated hopping and trap limited hopping models from computer simulation. Schmidline [24] proposed that the charge carrier transport process in amorphous solids could be explained by a model of multiple trapping levels, and Pollak [25] demonstrated theoretically that the dispersive transport can arise from a variety of distribution of different energy trapping sites. Noolandi [26] also suggested that only a few trapping levels would be necessary to explain the dispersive charge carrier transport process in disordered solids and that the multiple-trapping level model was equivalent to the time-dependent random-walk. Fleming [27] examined to solve numerically the transient photocurrent behaviors in dielectrics for the case of a continuous distribution of trap levels, and Demura et al. [28] also attempted an analysis of the transient photocurrent shape based on a trap-limited model by computer simulation.

Most of these analyses mentioned above did, however, go

into rather abstract arguments on carrier transport phenomena, and did not enter into discussions on the origin or nature of carrier traps which play an essential role in carrier transport process. Recently, Slowik et al. [29] proposed the idea of a conformational trap in PVCz from the calculation of the transfer integral between adjacent carbazole molecules with various orientations. Abkowitz et al. [30] discussed that structural fluctuations arising from molecular dynamic phenomena characteristic to the glass transition process can impact the carrier transport process in amorphous solids. Thus, the nature of traps and the relationship between carrier transport process and molecular dynamics are one of the current subjects in amorphous polymers.

In this thesis the author studied the carrier transport process in amorphous photoconductive polymers selecting PVCz as the object of the investigation. This selection was made from the standpoint that this material has been already utilized in the organic photoreceptors and has been studied well so far from many points of view.

In chapter 1, the physical meaning of Gill's empirical equation was elucidated, which was introduced first in the PVCz and PVCz-TNF systems as mentioned above and was applicable widely in many systems of amorphous polymers. The relationship between the carrier transport and the glass transition phenomena was investigated. The origin for the main carrier trap in PVCz was

proposed.

In chapter 2, the trap-free drift mobility which corresponds to the microscopic drift mobility during the displacement of carriers from trap to trap, was studied. The inherent upper limit of the drift mobility in amorphous polymers was presented. The effect of disordered alignments in amorphous polymers on the drift mobility was discussed.

In chapter 3, a new idea of trap control was proposed from the observation of drift mobility enhancement of PVCz by adding a certain low-molecular weight compound as the second component. The result would provide an important technique to improve the sensitivity of the organic photoconductor for the practical use.

Chapter 1

Drift Mobility in Amorphous Photoconductive Polymers

1-1 Introduction

A number of studies have been made on charge carrier transport in amorphous photoconductive polymers [3-20]. Pulse photoconduction measurements revealed that the hole drift mobility of amorphous polymers is very small and of the order of 10^{-7} cm²/sec.V, and strongly depends on the field and temperature. The following Gill's empirical expression [5] has been widely accepted to describe its field and temperature dependencies of the drift mobility,

$$\mu = \mu_0 \cdot \exp\left(-\frac{E_0 - \beta\sqrt{F}}{k \cdot T_{\text{eff}}}\right) \quad (1-1)$$

$$1/T_{\text{eff}} = 1/T - 1/T_0. \quad (1-2)$$

Here, μ is the drift mobility at a given temperature T , μ_0 the drift mobility at a critical temperature T_0 at which the field dependence of the drift mobility disappears, E_0 the trap depth, β the Poole-Frenkel coefficient, and F the applied field.

In this equation, the effective temperature T_{eff} is introduced in the exponential term instead of real temperature T to explain

the temperature dependence of the drift mobility, where T_{eff} is related to the critical temperature T_0 by Eq. (1-2). Hence, T_0 is defined as the temperature at which T_{eff} becomes infinite.

Pfister [18] suggested the interrelation between T_0 and the glass transition temperature T_g of an amorphous glassy polymer. No clear interpretation for the physical meaning of T_0 has, however, been presented so far.

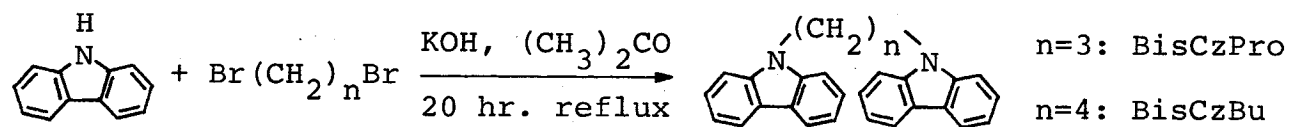
In the present work, the author found a clear correlation between T_0 and T_g in the typical photoconductive polymer, poly-N-vinylcarbazole (PVCz), doping with appropriate low-molecular weight model compounds, N-ethylcarbazole (EtCz), 1,3-bis-N-carbazolylpropane (BisCzPro) and 1,4-bis-N-carbazolylbutane (BisCzBu) shown in Fig. 1-1. In these systems it is possible to vary the glass transition temperature T_g by the plasticizing effect of the low-molecular weight compounds without changing the density of carbazole chromophores participating in the hole carrier transport.

1-2 Experimental

1-2-1 Sample

Commercially available PVCz, Luvican M170 (BASF), was purified by reprecipitations five times from a tetrahydrofuran-methanol system and then by Soxhlet extraction with hot methanol. EtCz was provided from Tokyo Kasei Co. Ltd. and recrystallized

two times from methanol. BisCzPro and BisCzBu were synthesized according to the following scheme [31];



and purified by recrystallizations two times from acetone before use.

The polymer films ($\approx 10 \mu\text{m}$) containing appropriate amount of the model compounds were prepared on a transparent nesa-coated glass electrode by solvent cast method, and were provided with an evaporated Au electrode on the free film surface to form a (nesa/polymer-film/Au) sandwich-typed cell assembly. The doping concentration of the low-molecular weight model compounds was varied within a range in so far as no microcrystals of the dopants separated.

1-2-2 Measurements

The hole drift mobility in these systems was measured by the time-of-flight technique illustrated in Fig. 1-2. For the exciting light source an N_2 gas laser (337 nm, pulse duration: 3 nsec, 50 μJ) was used. The positively biased electrode was irradiated. The induced photocurrent was recorded on an oscilloscope (Tektronix 5130N) with preamplification of 10 - 1000

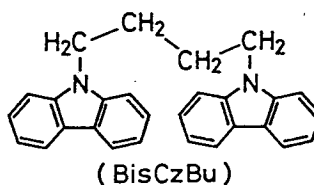
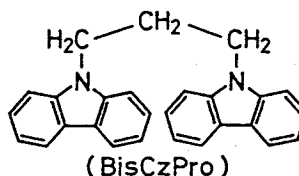
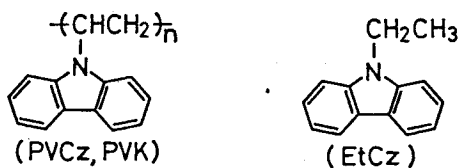


Fig. 1-1. PVCz and low-molecular weight model compounds of PVCz.

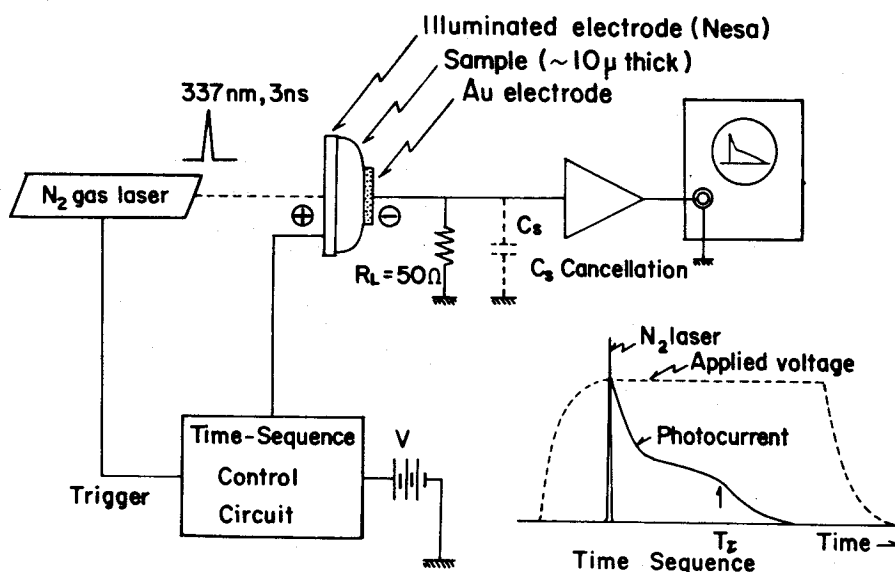


Fig. 1-2. Experimental scheme for the time-of-flight measurement using a sandwich-typed cell constructed of nesa/polymer-film/Au. A stray capacity cancellation circuit was inserted before the oscilloscope input and the voltage was applied only during the transient photocurrent measurement, for about 5 sec.

times. The load resistance was used in the range of 50Ω - $10 \text{ k}\Omega$. In measuring the fast decay of the photocurrent the cell directly connected to an oscilloscope (Tektronix 485) with input impedance of 50Ω . Minimum time constant of the measurement system was less than 50 nsec . The light intensity was adjusted carefully so as not to show a space charge perturbed current. The collected charge was estimated from the integration of the transient photocurrent curve. Measurements of temperature dependence were carried out after maintaining the sample film for several hours at each temperature. Photoconduction measurements were carried out in vacuo.

The glass transition temperature of each sample was determined by the DSC measurements (Daini Seikosha Model SSC-560).

1-3 T_0 in PVCz - Low-molecular Weight Model Compound Systems

Typical transient photocurrent curves are shown in Fig. 1-3. Fig. 1-4 shows a typical temperature dependence of the drift mobility for different applied fields in the PVCz-EtCz (1:0.1 mol) sample. The glass transition temperature T_g of this sample was 443 K . The drift mobility measured below T_g is expressed correctly by the Gill's empirical equation, i.e., Eq. (1-1). The critical temperature T_0 at which the field dependence vanishes, was 558 K . The experimental error in the estimation of

Fig. 1-3. Typical transient photo-current curves of PVCz in various fields. Sample thickness: 6 μm ; measured at 294 K.

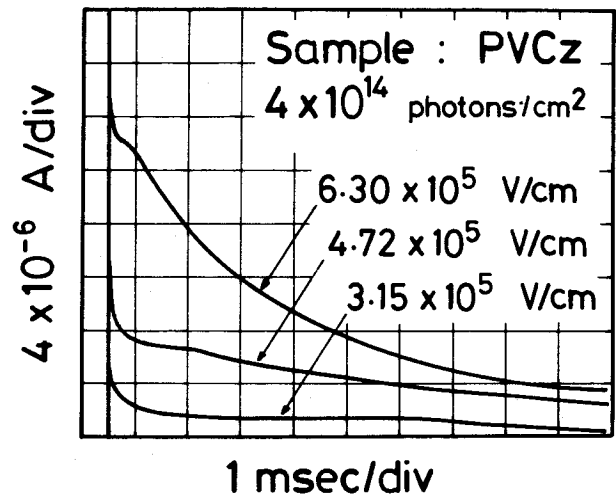
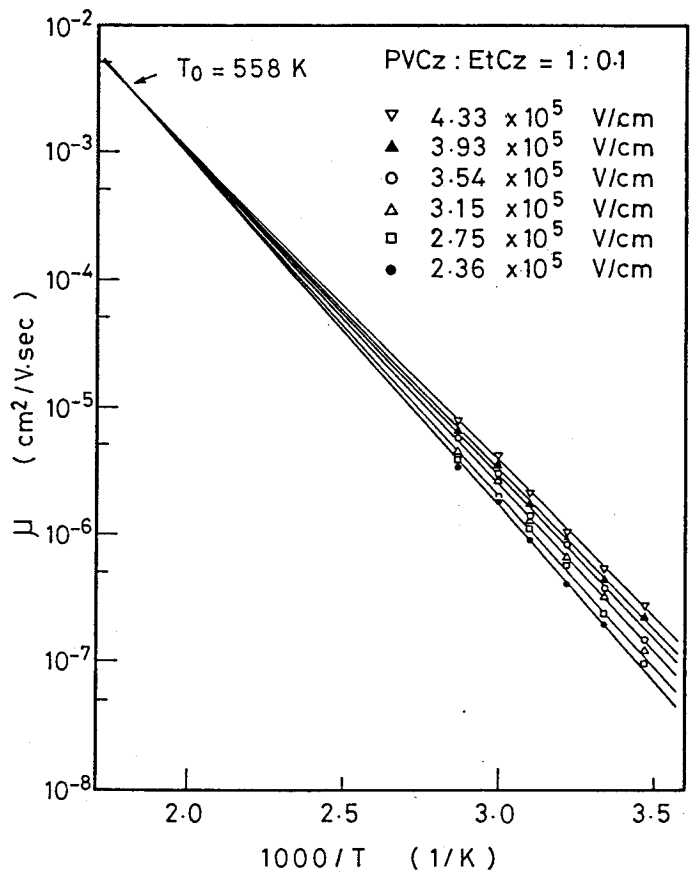


Fig. 1-4. Temperature dependence of the hole drift mobility with the applied field as a parameter in a PVCz-EtCz (1:0.1 mol) film. The values of T_0 and μ_0 obtained show a remarkable lowering from those of a neat PVCz film.



T_0 values was within about ± 30 K. The values of μ_0 , E_0 , and β were obtained as $3.25 \times 10^{-3} \text{ cm}^2/\text{sec.V}$, 0.70 eV , and $3.24 \times 10^{-4} \text{ eV(V/cm)}^{-1/2}$, respectively. These values of E_0 and β are acceptable as compared with those for a neat PVCz sample [5,32], indicating that the dopants do not seriously affect the hole transport properties. However, it can be seen that both T_0 and μ_0 in this sample show remarkable lowering from the values of 653 K and $10^{-2} \text{ cm}^2/\text{sec.V}$ obtained in PVCz [5,32], respectively. In Table 1-I are listed the values of T_0 and μ_0 in the PVCz-EtCz systems. As the EtCz concentration increases, T_0 decreases gradually.

In Fig. 1-5 are plotted the T_0 and T_g values as a function of the EtCz concentration. T_g decreases gradually with the increase of EtCz concentration due to the plasticizing effect as expected. As can be seen from this figure, the tendency of lowering of T_0 is quite parallel with that of T_g , showing the difference of about 100 K between T_0 and T_g . The same dependence was observed in other systems, e.g., PVCz-BisCzPro or PVCz-BisCzBu systems as shown in Figs. 1-6 and 1-7. These results would strongly suggest that T_0 is closely related to T_g in that the temperature T_0 is so-to-say a 'glass transition temperature in the hole carrier transport phenomena'.

Table 1-I
EtCz concentration dependence of T_g and T_0 .

PVCz : EtCz (mol : mol)	T_g (K)	T_0 (K)	μ_0 ($\text{cm}^2/\text{sec}\cdot\text{V}$)	E_0 (eV)	β ($\text{eV}/\text{cm})^{-1/2}$)
1 : 0	498	630	7.58×10^{-3}	0.67	3.46×10^{-4}
1 : 0.10	443	558	3.25	0.70	3.24
1 : 0.25	408	504	1.00	0.74	3.80
1 : 0.50	306	412 ± 10	$1.56 \pm 0.16 \times 10^{-4}$	0.95 ± 0.12	5.38 ± 1.57
1 : 0.70	263	367 ± 20	$2.87 \pm 1.37 \times 10^{-5}$	0.97 ± 0.06	5.41 ± 1.08

μ_0 : Drift mobility at T_0 .
 E_0 : Activation energy at zero field.
 β : Poole-Frenkel coefficient.

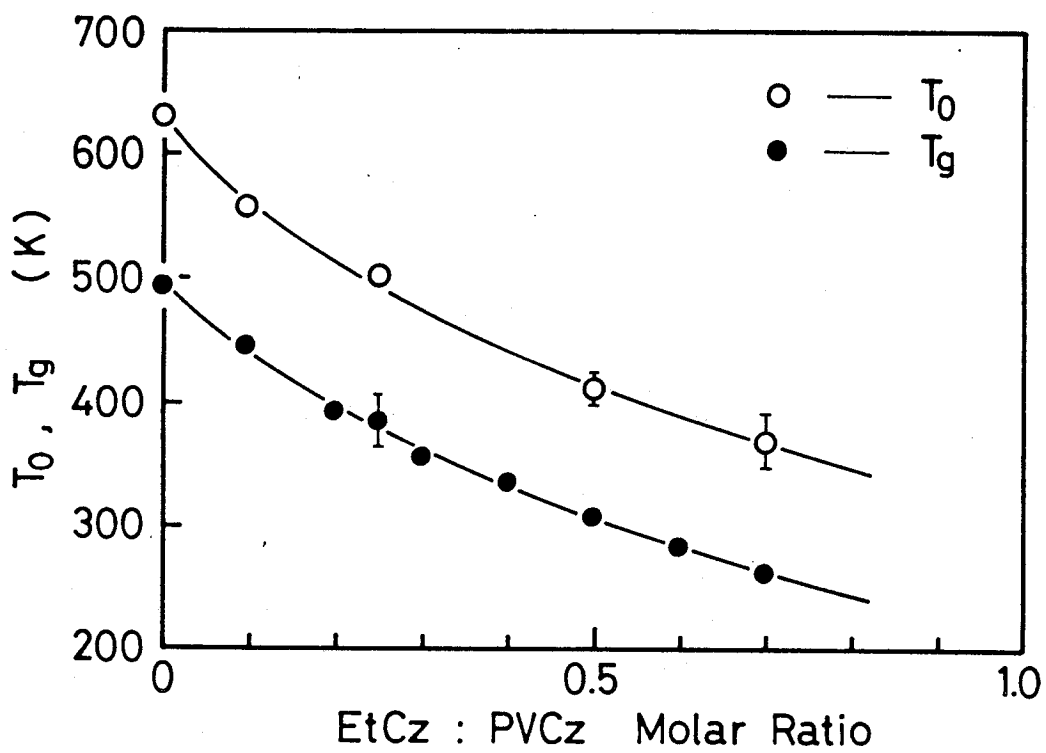


Fig. 1-5. Variation of the critical temperature T_0 and the glass transition temperature T_g as a function of EtCz concentration in the PVCz-EtCz system.

Fig. 1-6. Variation of T_0 and T_g as a function of BisCzPro concentration in the PVCz-BisCzPro system.

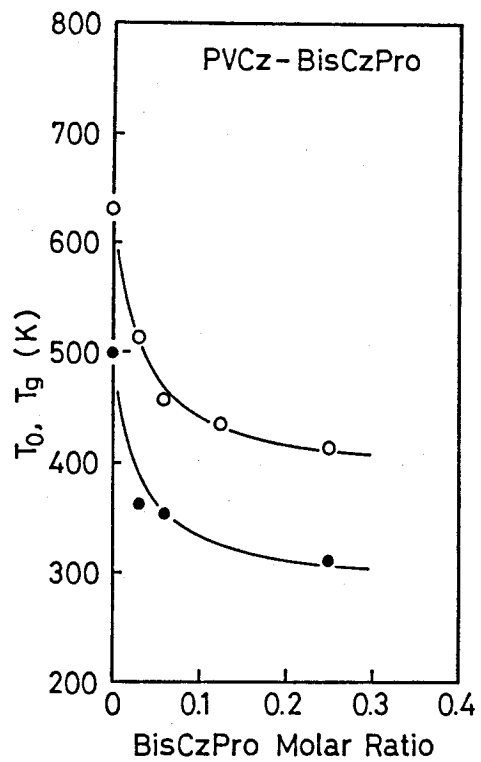
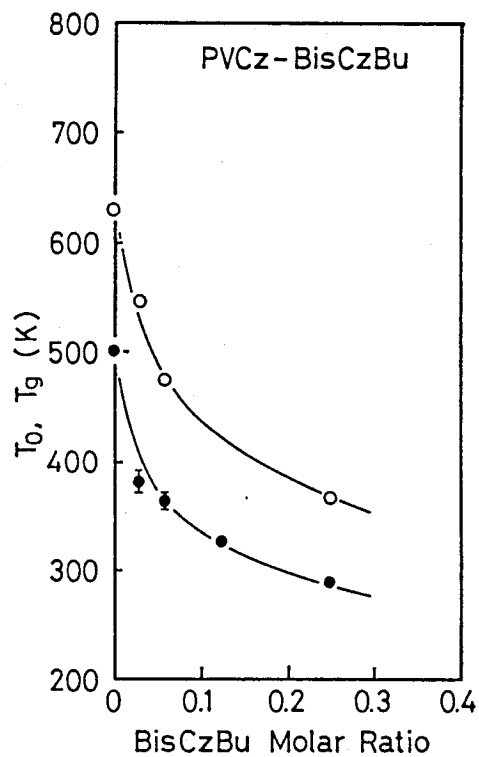


Fig. 1-7. Variation of T_0 and T_g as a function of BisCzBu concentration in the PVCz-BisCzBu system.



1-4 T_0 and Segmental Motion

As the mechanism of charge carrier transport in amorphous glassy polymers the hopping conduction from trap to trap is usually considered. The depth E_0 of the traps for the hole carrier in PVCz, which controls the hopping conduction in the carrier transport, has been reported to be about 0.65 eV [5]. From the result shown in Fig. 1-4, 0.70 eV was obtained for E_0 . If the trap in PVCz is due to the structural trap, it might be expected that the change of the thermodynamical state such as glass transition would be reflected on the properties of the charge carrier transport. For such a structural trap, the author considers the excimer-forming (or dimer) site in which the planes of two pendant carbazole chromophores are arranged parallel to each other. The existence of such dimer sites in a solid film has been established to be about 10^{-3} mol/mol unit from the observation of the excimer fluorescence [33]. The hole carrier on the dimer site would be in a dimer radical cation state which is expected to be more stable than the radical cation on the single carbazole ring, i.e., an isolated hole carrier.

In the glassy state below T_g , the segmental motion is frozen and therefore the detrapping of the trapped carriers is ascribed to the field-assisted thermal activation. The drift mobility in PVCz below T_g , therefore, strongly depends on the temperature and applied field, resulting in the Poole-Frenkel type detrapping. Above T_g , the segmental motion begins to occur to convert the

system into the supercooled liquid state with high viscosity. However, since even above T_g , segmental motion below T_0 is expected to be so insufficient for the hole carrier detrapping phenomena, it will be understood that the drift mobility in PVCz still depends on temperature and applied field resulting in the Poole-Frenkel type detrapping up to T_0 . For the detrapping process of the trapped carriers in the supercooled liquid state above T_0 , the segmental motion would be more effective, which forces to convert the trapped hole, i.e., dimer cation radical state, into free hole, i.e., an isolated cation radical state as illustrated in Fig. 1-8. Therefore, the Poole-Frenkel effect would no longer be observed above T_0 . Since this state is sufficiently in thermodynamical equilibrium with the environments, not the effective temperature T_{eff} based on the critical temperature T_0 but real temperature T would be operative.

As mentioned above, there exists the difference of about 100 K between T_0 and T_g . This difference is considered to be the excess thermal energy necessary to make the time scale of the segmental motion comparable to the trapping time. When the time scale of the segmental motion become shorter than the trapping time at the dimer site, the trapped carrier would be detrapped by the dynamic motion of the segment. Pfister [18] reported the difference between T_0 and T_g in a molecularly dispersed photoconductor, i.e., triphenylamine (TPA)-polycarbonate (PC) system, in which the difference between T_0 and T_g is much smaller than the present system. In TPA-PC system the TPA molecule

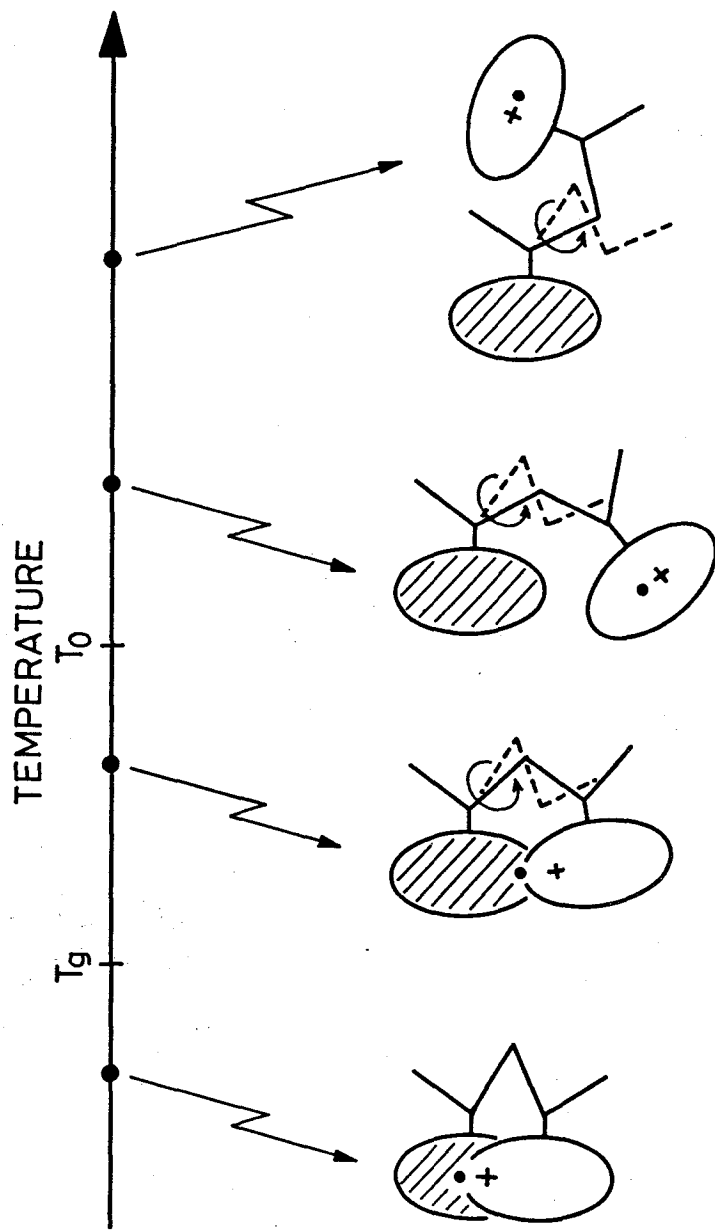


Fig. 1-8. Structural trap in PVCz and carrier detrapping processes.

taking the part of the carrier transport is free from the polymer chain and can take any dynamical motion above T_g , while in PVCz the carbazole ring is tightly connected to the backbone chain and is limited from rotation. Such difference in both systems might be reflected on the difference between T_0 and T_g .

1-5 Relationship between T_0 and μ_0

As expressed in Eq. (1-1), μ_0 is the drift mobility at T_0 . The μ_0 values decrease gradually with increasing EtCz concentration. As shown in Fig. 1-9, a straight line is obtained in the Arrhenius plot of μ_0 against $1/T_0$. From the slope, the activation energy was obtained as 0.4 eV. As shown in the same figure, very interestingly, the μ_0 values obtained in the different systems with different doping concentration of BisCzPro, BisCzBu and with light doping of TNF (2,4,7-trinitrofluorenone) [5] lie on a same straight line. Since μ_0 is the drift mobility at T_0 , namely, at the transition temperature from the glassy state to the supercooled state, the slope of this straight line represents the activation energy for the hole carrier transport in the supercooled liquid state of PVCz itself.

This consideration is confirmed by measuring the drift mobility in the sample of PVCz-EtCz (1:0.7 mol) over a wide temperature range covering the T_0 temperature in between. The rather low glass transition temperature ($T_g = 263$ K) of this

Fig. 1-9. Arrhenius plot of μ_0 against $1/T_0$ in various PVCz-model compound systems. The figures indicated represent the doping molar ratio. The activation energy of about 0.4 eV was obtained from the slope.

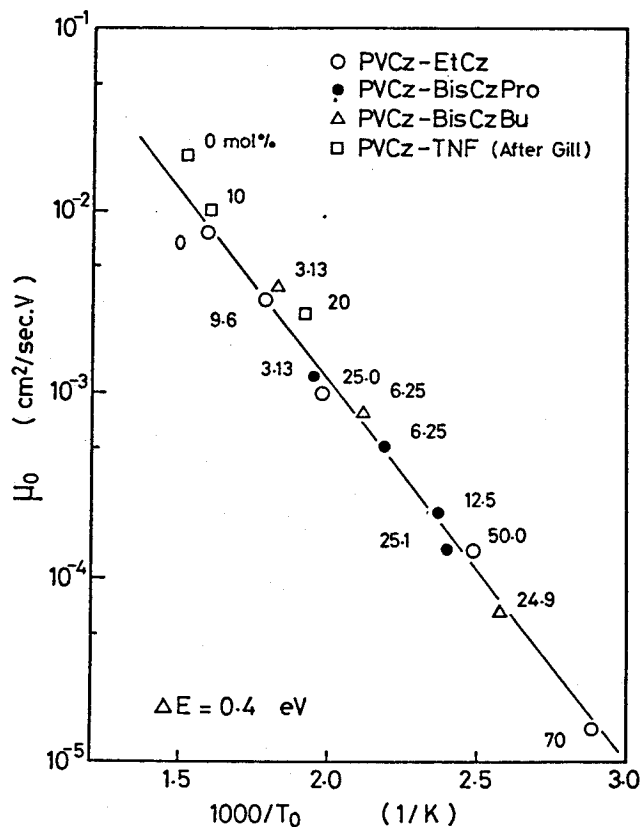
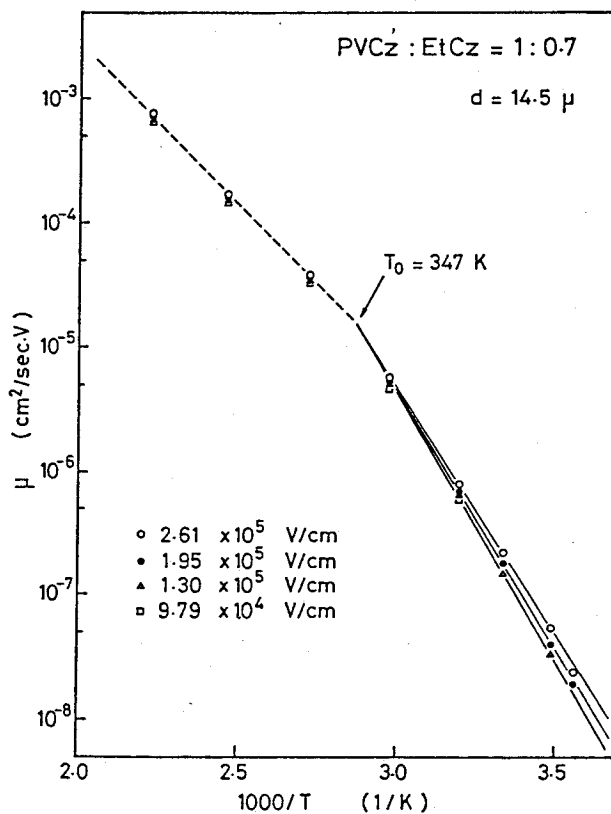


Fig. 1-10. Temperature dependence of the hole drift mobility with the applied field as a parameter in a PVCz-EtCz (1:0.7 mol) film. Below T_0 (347 K) the well-defined Poole-Frenkel effect was observed and above T_0 , the drift mobility is independent of the field.



sample makes the measurements easier. The result is shown in Fig. 1-10. Below T_0 the well-defined Poole-Frenkel type field dependence was observed according to Eq. (1-1). Above T_0 , however, the drift mobility followed a beautiful single straight line regardless of the different applied fields. The slope of the line gave 0.5 eV as the activation energy well corresponding to the value obtained in a $\log(\mu_0)$ vs. $1/T_0$ plot of Fig. 1-9.

1-6 Annealing Effect

The annealing effect on the glass transition temperature T_g is well-known in polymers. Therefore, the annealing effect should be appeared on the critical temperature T_0 and other transport properties. In this section, the effect of heat treatments was examined.

In Fig. 1-11 are shown the DSC thermograms of the sample (PVCz:EtCz = 1:0.7 mol) for the first scan (virgin sample) and the second scan (annealed sample) after heated up to 470 K with heating rate of 20 K/min, for instance. The T_g of this sample was 263 K in the first scan, while 313 K was observed in the second scan and in successive measurements after the second scan the same transition temperature was obtained in well-reproduced thermograms. The similar behavior was observed in other dopant concentration as well as in other model compound systems. The DSC curves for the various concentration of EtCz measured in the

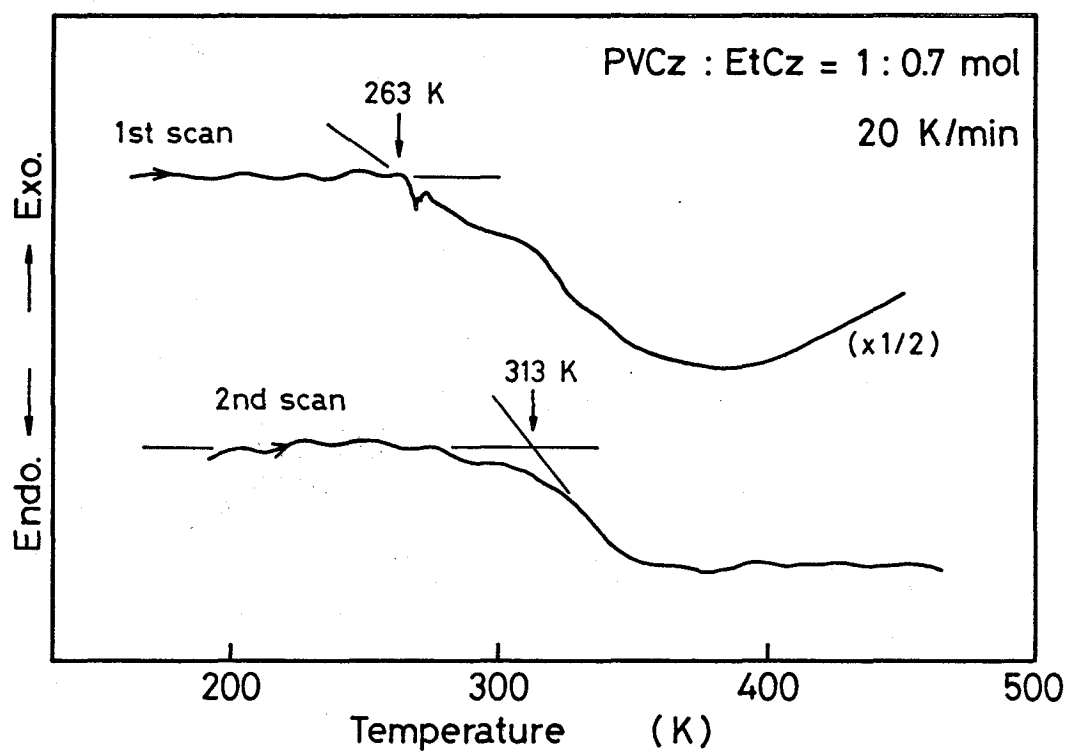


Fig. 1-11. DSC thermograms of PVCz-EtCz (1:0.7 mol) film with heating rate of 20 K/min. The glass transition temperature obtained in the second heating process is higher than that obtained in the first heating process.

second scan are shown in Fig. 1-12. The DSC thermograms in the second scan gave the relatively well-defined endothermic base line shift due to the glass transition. In Fig. 1-13 are compared the glass transition temperatures for the virgin and heat-treated samples as a function of EtCz concentration. The annealing effect is much predominant in the samples of high EtCz concentration. T_g of the annealed samples, however, decreases with the increase of EtCz content due to the plasticizing effect.

T_0 of the annealed samples also shifted to the higher temperature as listed in Table 1-II. The shifts of T_g and T_0 by the heat treatment are quite parallel, providing another evidence for the correlation of T_g and T_0 discussed above.

In Table 1-III are compared the drift mobilities μ at room temperature for the virgin and annealed samples of three different EtCz concentration. The annealed samples gave the larger value of μ than the each virgin sample, and the large annealing effect was also recognized in the samples of high EtCz content.

These observations mentioned above are considered due to the conformational change of PVCz itself or much more due to the change in the spatial alignment of dopant molecules. A large number of unstable spatial alignments of dopant molecules in a polymer matrix would exist in a solvent cast film (virgin sample). These unstable alignments would be converted to the more stable position and orientation by heat treatment above T_g . Such a small displacement of the dopant molecules would

Fig. 1-12. DSC thermograms of PVCz-EtCz film for different EtCz concentration.

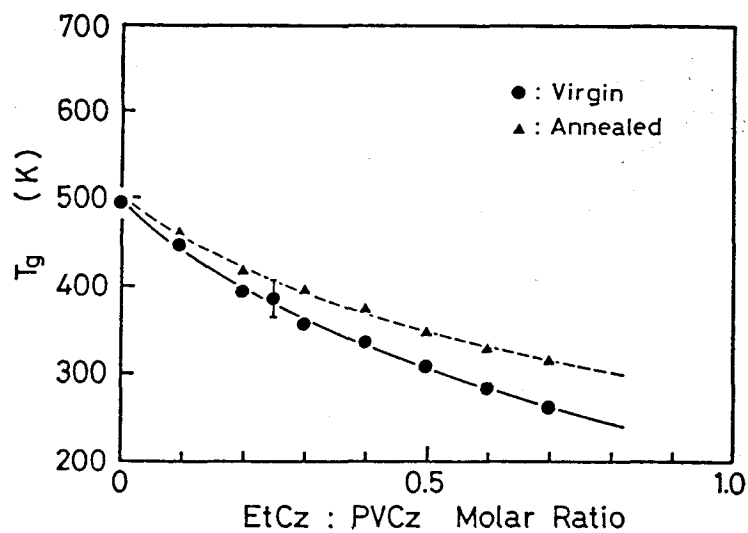
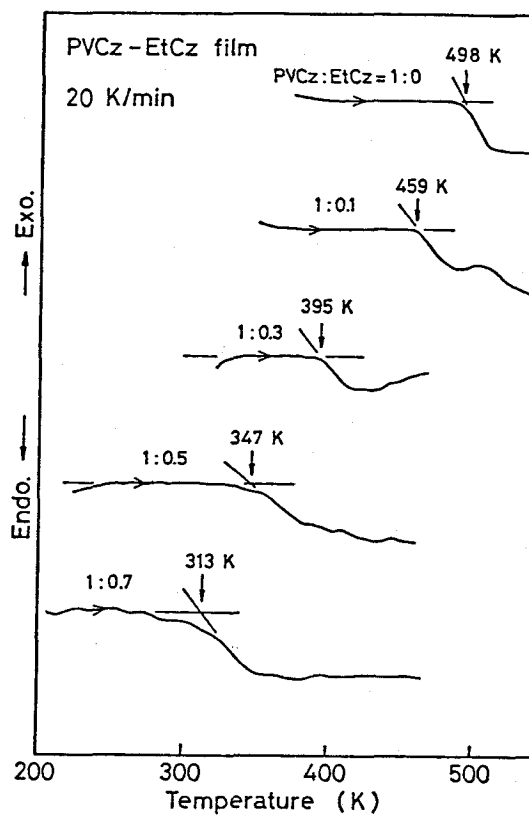


Fig. 1-13. EtCz concentration dependence of the glass transition temperature T_g . Solid curve shows T_g of virgin sample and broken curve shows T_g of annealed sample.

Table 1-II
 T_0 temperatures of virgin and annealed samples
in PVCz-EtCz systems.

PVCz : EtCz (mol : mol)	T_0 (K)	
	virgin	annealed
1 : 0.5	423	444
1 : 0.7	388	431

Film thickness : $\approx 9 \mu\text{m}$.

Table 1-III
Hole drift mobilities of virgin and annealed samples in
PVCz - EtCz systems.

PVCz : EtCz (mol : mol)	μ ($\text{cm}^2/\text{sec.V}$)	
	virgin	annealed
1 : 0.25	1.9×10^{-7}	2.9×10^{-7}
1 : 0.50	3.9×10^{-7}	7.0×10^{-7}
1 : 0.70	4.9×10^{-7}	2.2×10^{-6}

Measured at room temperature.
Applied field: 5×10^5 V/cm, film thickness: $\approx 9 \mu\text{m}$.

begin to occur just below the glass transition temperature. This gave rise to the unstable base line in the DSC thermogram of the first scan.

The existence of the unstable alignments of dopant molecules in a solvent cast film can be confirmed in the thermally stimulated current (TSC) measurements. Fig. 1-14 shows the TSC curves of the PVCz-EtCz (1:0.7 mol) system. Comparison between the first and second measurements clearly shows the great change in the trap distribution. The wide energy distribution of trap level in the virgin sample disappeared by annealing, and a discrete trap level characteristic to PVCz, which usually gives a TSC peak at about 260 K with activation energy of about 0.6 eV remained unchanged.

Thus, the annealing effect would bring the high temperature shift of T_g and therefore, of T_0 as an expected consequence.

1-7 Conclusion

In this chapter the physical meaning of Gill's empirical equation was investigated.

(1) The author found a clear correlation between T_0 and T_g in the amorphous glassy photoconductive polymers, and suggested that T_0 is the transition temperature from the amorphous glassy state to the supercooled liquid state in the hole carrier transport phenomena at which the carrier detrapping

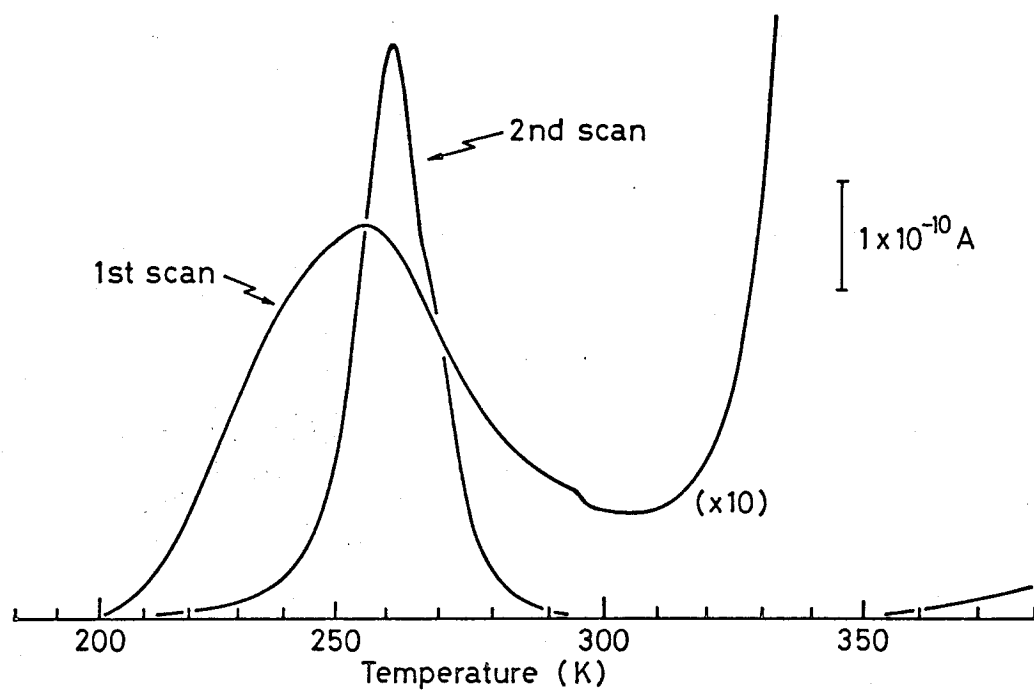


Fig. 1-14. TSC curves in PVCz-EtCz (1:0.7 mol) system at 1×10^5 V/cm. Heating rate: 8 K/min; sample thickness: 8 μm . Carriers were generated at 185 K with 340 nm irradiation of xenon lamp under 1×10^5 V/cm.

mechanism is changed. The observed temperature difference between T_0 and T_g comes from the thermal energy necessary for the sufficient segmental motion to convert the dimer cation radical state as a trapped hole carrier into a free isolated cation radical and a neutral moiety.

(2) It was shown that μ_0 represents the drift mobility at the transition temperature T_0 from the glassy state to the supercooled state.

(3) It was also shown that the structural defect, i.e., dimer site, characteristic of amorphous polymers is a prominent candidate as an important carrier trap of PVCz which makes the hole drift mobility lower.

Chapter 2

Trap-Free Drift Mobility in Amorphous Photoconductive Polymers

2-1 Introduction

The charge carrier transport in amorphous organic materials is one of the current subjects from the viewpoint of the practical use of organic photoconductors. The transport process of the charge carriers in such amorphous materials generally involves a thermally activated hopping conduction from trap to trap [3-20].

The values of the drift mobility in photoconductive organic crystals of low-molecular weight compounds have been reported in the range from 1 to 10^{-3} $\text{cm}^2/\text{sec.V}$ [20,34], while in amorphous glassy and supercooled liquid states of the same compound much lower drift mobilities have been reported. In a pyrazoline derivative, for example, the disorder of molecular alignments in the amorphous glassy state reduces the hole drift mobility by about three orders from the value in the single crystal state [20]. In amorphous selenium, the similar order of lowering in the drift mobility was reported as compared with the case of its single crystal [6]. On the other hand, the drift mobility of the amorphous polymers, poly-N-vinylcarbazole (PVCz), for instance, is the order of 10^{-7} $\text{cm}^2/\text{sec.V}$ with strong dependences on the applied electric field and temperature [5]. There exists much

larger drop of the drift mobility in PVCz when compared with the value, about $0.1 \text{ cm}^2/\text{sec.V}$, of a single crystal of N-isopropylcarbazole, i.e., a low-molecular weight model compound [34]. Such a large change of about 6 orders seems to be caused by a number of traps existing in PVCz in addition to the disorder of the molecular alignments in the amorphous state. From the thermally stimulated current measurements [35], the density of the trapping sites governing charge carrier transport in this material has been reported to lie in the range from $10^{16} - 10^{18} \text{ cm}^{-3}$, which gives a few hundred angstroms as the average distance of such trapping sites. One may imagine that the charge carriers can drift much faster through the pendant carbazole rings of about 100 pieces from one trapping site to the next site. Here, we define the trap-free drift mobility μ_f as the drift mobility of the charge carriers traveling among the trapping sites.

The concept of the drift mobility under trap-free condition was first reported by Hughes [36], and recently recognized by Reimer et al. [37] and Hirsh [38].

In this chapter, the author attempted to estimate the trap-free drift mobility in PVCz from the transient photocurrent value directly by introducing the concept of the thermal equilibrium between trapped and free carriers. A value of about $1 \times 10^{-3} \text{ cm}^2/\text{sec.V}$ was obtained as the trap-free drift mobility in this polymer with a small temperature dependence with an activation energy of about 0.1 eV. The carrier transport mechanism under trap-free condition was also discussed.

2-2 Method of Analysis

In the present analysis the charge carrier transport in PVCz is considered to be controlled by trapping and thermal detrapping processes. A hole carrier trap having about 0.5 eV as the trap depth is reported to be operative from the transient photocurrent [5] and thermally stimulated current [35] measurements. In previous chapter, this carrier trap was found to be the structural defect, and the dimer site arising from the characteristics of vinyl polymers was shown to be the most plausible candidate.

As the dimer structure has a specific conformation, a single discrete trap level can be considered to be operative in carrier transport of PVCz as the first approximation. Then the following equation holds for the detrapped, i.e., free, carrier density, n_f ;

$$\frac{dn_f}{dt} = \frac{n_t}{\tau_t} - \frac{n_f}{\tau_f} \quad (2-1)$$

where τ_f is the lifetime of free carriers, τ_t the lifetime of trapped carriers, and n_t the number of trapped carriers.

In a time-of-flight measurement, the induced photocurrent, $I_{\text{obs}}(t)$, observed at a given time t is proportional only to the number of free carriers, n_f , which can drift at that time. Introducing the trap-free drift mobility, μ_f , for the free carrier, $I_{\text{obs}}(t)$ is written as follows.

$$I_{\text{obs}}(t) = (l/d) \cdot e \cdot n_f \cdot \mu_f \cdot F \quad (2-2)$$

Here, d is the sample thickness, e the electronic charge, and F the applied field. Solving Eq. (2-1) for n_f under the initial condition of $n_f = n_0$ at $t = 0$, where n_0 is the total charge carrier produced by the light irradiation, Eq. (2-2) leads to the following expression.

$$I_{\text{obs}}(t) = \frac{1}{d} \cdot e \cdot \mu_f \cdot F \cdot n_0 \cdot \left[\frac{\tau_t}{\tau_f + \tau_t} \cdot \exp\left\{-\left(\frac{1}{\tau_f} + \frac{1}{\tau_t}\right)t\right\} + \frac{\tau_f}{\tau_f + \tau_t} \right] \quad (2-3)$$

The first exponential term in the brackets in Eq. (2-3) represents the transient process to a steady state of trapping and detrapping processes, and is dominant at small t . The second term shows the thermal equilibrium of trapping and detrapping processes, and indicates that only free carriers contribute to the photocurrent at any given time. Since τ_t is much larger than τ_f , as is assumed generally, implying that the number of trapped carriers, n_t , is much larger than that of free carriers, n_f , the second term can be replaced by the ratio of trapped and free carriers:

$$\tau_f / (\tau_f + \tau_t) \approx n_f / n_t \quad (2-4)$$

Here, one may introduce the following relation into this ratio;

$$n_f / n_t = \exp(-E_a/kT) \quad (2-5)$$

where E_a is the activation energy for detrapping from the trap. As discussed in a previous chapter, in amorphous glassy polymers, it seems reasonable to employ the effective temperature expressed by the following equation:

$$1/T_{\text{eff}} = 1/T - 1/T_0 \quad (2-6)$$

Here, T_0 is the temperature at which the field dependence of the overall drift mobility vanishes. Thus, we adopt the following Boltzmann distribution with T_{eff} instead of real temperature T to evaluate the ratio n_f/n_t :

$$n_f / n_t = \exp(-E_a/kT_{\text{eff}}) \quad (2-7)$$

In evaluating E_a , the Poole-Frenkel type of barrier lowering [39] was taken into account, i.e.,

$$E_a = E_0 - \beta\sqrt{F} \quad (2-8)$$

The first term in Eq. (2-3) is negligible at sufficiently large time, at which the transient photocurrent curve gives an apparent plateau. Hence, $I_{\text{obs}}(t)$ can be reduced to,

$$I_{\text{obs}}(t) = (1/d) \cdot e \cdot \mu_f \cdot F \cdot n_0 \cdot \exp(-E_a/kT_{\text{eff}}). \quad (2-9)$$

Hence, the number of total carriers, n_0 , can be obtained from the

integration of the transient photocurrent. Other variables are also obtainable under the experimental conditions. Thus, the trap-free drift mobility, μ_f , can be estimated by this equation.

2-3 Evaluation of μ_f and Field Dependence

To evaluate μ_f from the transient photocurrent $I_{obs}(t)$, the current value $I_{d/2}$ at $t = t_\tau/2$ (t_τ : transit time) was used, since at $t = t_\tau/2$, most of the carriers would pass the halfway point of the sample and thermal equilibrium of trapping and detrapping of carriers would be attained. The E_a values for various field strengths were calculated from Eq. (2-8) by using the values, $E_0 = 0.68$ eV, $\beta = 2.72 \times 10^{-4}$ eV(V/cm) $^{-1/2}$, $T_0 = 660$ K, referring Gill's data [5]. The values of μ_f were evaluated using the values, $I_{d/2}$, n_0 , E_a for each electric field and T_{eff} given by Eq. (2-6). The results are listed in Table 2-I. The values of about 1×10^{-3} cm²/sec.V was obtained, being almost field-independent. This value is about 10^4 times larger than the overall drift mobility of about 10^{-7} cm²/sec.V, and gives fairly good agreement with those reported by Hughes [36], Reimer et al. [37] and Hirsh [38], who also attempted to estimate by different experimental methods.

The μ_f value obtained is smaller by about two or three orders as compared with the drift mobility in an N-isopropylcarbazole single crystal [34]. This difference gives fairly good agreement

Table 2-I
Calculation of Trap-Free Drift Mobility μ_f .

F (V/cm)	a) $I_{d/2}$ (A)	b) n_0	c) n_f	d) μ_f ($\text{cm}^2/\text{sec}\cdot\text{V}$)
3.15×10^5	9.08×10^{-9}	6.68×10^9	1.09×10^5	9.84×10^{-4}
3.93	2.40×10^{-8}	1.11×10^{10}	2.68	8.49
4.72	4.96	1.62	5.62	6.92
5.50	1.09×10^{-7}	2.17	1.05×10^6	7.02
6.30	2.29	2.92	1.93	7.00

a) Observed Photocurrent value at $t = t_T/2$.

b) Obtained from the integration of transient photocurrent.

c) Calculated using Eqs. (2-7) and (2-8) in the text; $E_0 = 0.65 \text{ eV}$, $\beta = 2.72 \times 10^{-4} \text{ eV(V/cm)}^{-1/2}$, $T_0 = 660 \text{ K}$, $T = 292 \text{ K}$.

d) Calculated from Eq. (2-9) in the text.

with the value obtained from the comparison between glassy and single crystal states of pyrazoline derivative [20]. It will be concluded that the disorder of molecular alignments reduces the drift mobility only by two or three orders from that of single crystal state. The trapping process at the sites of about 0.5 eV trap depth makes the overall drift mobility of PVCz to the order of 10^{-7} cm²/sec.V. If the such deep traps in PVCz are externally controlable, we would expect a high drift mobility near 10^{-3} cm²/sec.V.

Figure 2-1 shows a rough sketch of transient photocurrent profiles based on the idea that μ_f is independent of the field strength. As the field increases, $I_{d/2}$ increases. This can be considered due to an increase in free carrier density n_f arising from an increase in total carrier (n_0) yield and the Poole-Frenkel barrier lowering under applied fields, but not due to the field-dependence of drift mobility itself.

2-4 Initial Peak Current

As can be seen in Fig. 1-3, a spike-like photocurrent is observed at the initial time region of the transient photocurrent of PVCz. Hughes [40] analyzed this peak current based on the recombination theory in PVCz-TNF (2,4,7-trinitrofluorenone) system and Reimer et al. [37] attempted to analyze the initial photocurrent in terms of thermal diffusion of injected carrier

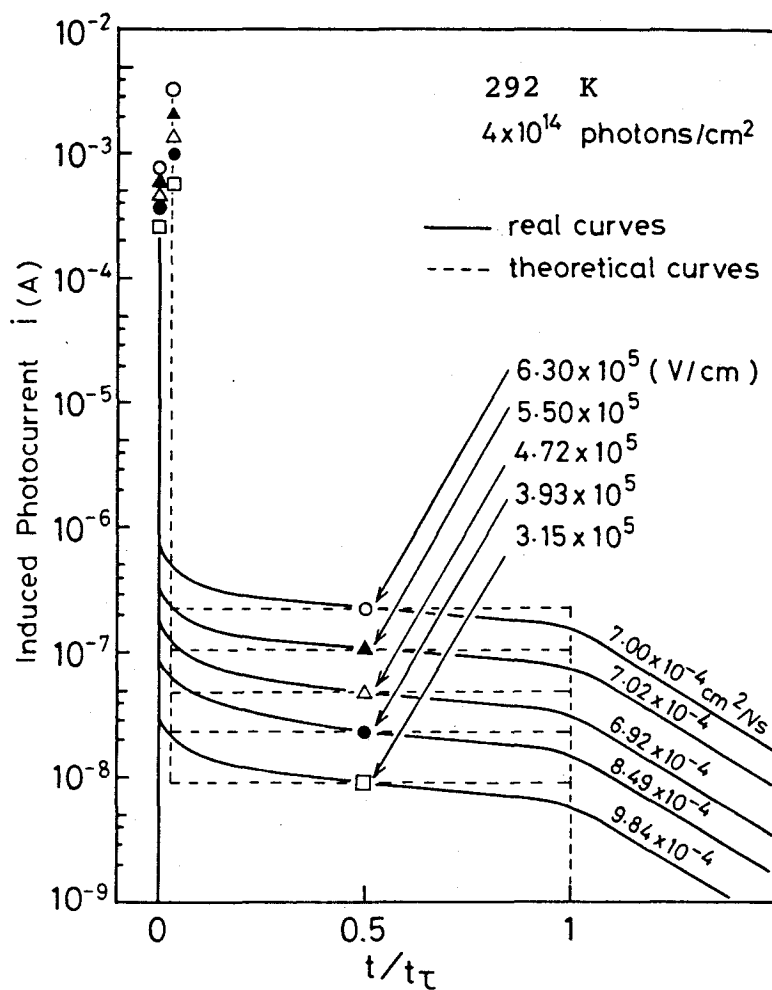


Fig. 2-1. Field dependence of transient photocurrents in PVCz. The solid and broken curves represent the observed and theoretical curves, respectively. Applied fields: as indicated; time axis is normalized by transit time t_τ ; sample thickness: 6 μm ; measured at 292 K in vacuo.

sheet in Se-PVCz double layered system. The author analyzed the spike-like photocurrent peak under the consideration of the trap-free conduction of hole carriers.

In the initial nonequilibrium state, only the first term in Eq.(2-3) is predominant, and therefore, all the photocarriers produced can move toward the counter electrode. The initial peak current values are evaluated using a constant μ_f and respective n_0 values at various fields. As shown in Fig. 2-1, the results are in good agreement with the experimental data. This indicates that a large current drop subsequent to the initial photocurrent peak is caused mainly by transient trapping process before the thermal equilibrium state of trapped and detrapped carriers is attained.

Above result shows the validity of the present analysis based on the thermal equilibrium in carrier transport represented by Eq. (2-3) and the value obtained, i.e., $10^{-3} \text{ cm}^2/\text{sec.V}$ is also shown to be reasonable as the trap-free drift mobility μ_f .

2-5 Temperature Dependence of μ_f

The trap-free drift mobility μ_f obtained in a previous section is about $10^{-3} \text{ cm}^2/\text{sec.V}$ larger than the overall drift mobility of $10^{-7} \text{ cm}^2/\text{sec.V}$. The carriers under trap-free condition should be transported by different mechanism from that of usual process discussed for the overall drift mobility.

In order to interpret the transport process under trap-free condition, the temperature dependence of μ_f evaluated by using Eq. (2-9) was also examined.

The Arrhenius plots of the drift mobility obtained from the transient photocurrent curves in PVCz are shown in Fig. 2-2, which show the similar feature as Gill's results. The parameters in Gill's empirical expression obtained in the present sample are essentially the same as those reported by Gill [5] within the experimental errors, as shown in Table 2-II.

In Fig. 2-3 are shown the Arrhenius type of plots of μ_f . The values obtained ranged within the order of 10^{-3} cm²/sec.V, showing a significant tendency of a gradual increase with increasing temperature. A small value of about 0.1 eV was obtained for the activation energy (ΔE) at a constant applied field of 5×10^5 V/cm. This result suggests that under the trap-free condition there still exists a small thermally activated process with an activation energy ΔE for the carrier transport in PVCz. This will be discussed later.

In Fig. 2-4 is shown the applied field dependence of the activation energy ΔE in μ_f . The ΔE does not show any significant field dependence as is generally observed in overall drift mobility μ , in which the Poole-Frenkel type of barrier lowering is appeared as expressed in Eq. (2-8), and an average value of 0.12 eV was obtained. This value for the trap-free condition seems to be close to the activation energy of 0.06 eV in N-isopropylcarbazole single crystal [34]. A slightly large value

Fig. 2-2. Temperature dependence of hole drift mobility with applied field as a parameter in a PVCz film.

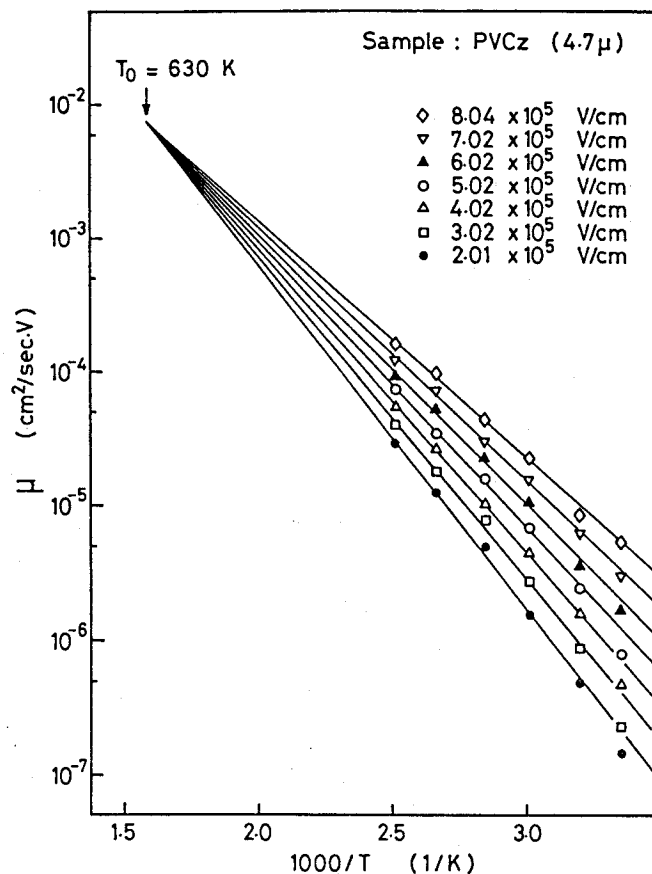


Table 2-II
Parameters in Gill's empirical expression* obtained from the present experiment.

T_0 (K)	μ_0 ($\text{cm}^2/\text{sec.V}$)	E_0 (eV)	β ($\text{eV}(\text{V}/\text{cm})^{-1/2}$)	
630	7.6×10^{-3}	0.67	3.46×10^{-4}	This work
660	2×10^{-2}	0.65	2.72×10^{-4}	Ref. [5]

* $\mu = \mu_0 \exp[-(E_0 - \beta\sqrt{F})/kT_{\text{eff}}]$.

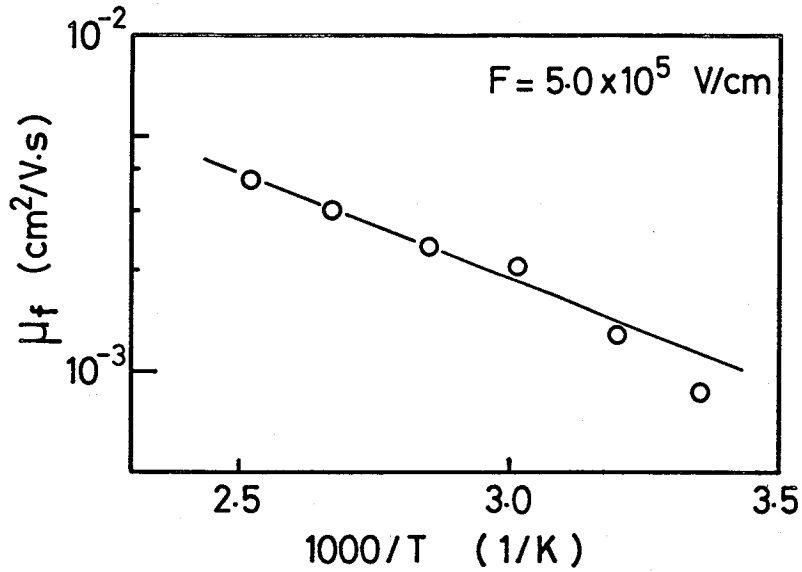


Fig. 2-3. Temperature dependence of trap-free drift mobility at $F = 5 \times 10^5$ V/cm in a PVCz film. The activation energy of about 0.1 eV was obtained in this case.

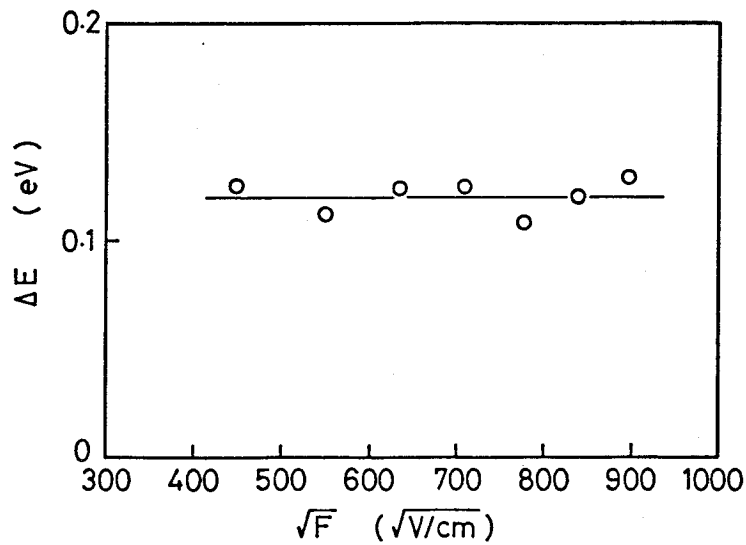


Fig. 2-4. Activation energies of trap-free drift mobility as a function of applied field in a PVCz film. No field dependence was shown and the average value of 0.12 eV was obtained.

in PVCz is considered to be originated from the low orientation of chromophores in the amorphous state. The value of 0.12 eV is happen to be the same as the activation energy reported by Szymanski et al. [41], who once observed highest overall drift mobility of the order of 10^{-3} cm²/sec.V in PVCz so far. This result would make us imagine that they happened to measure the drift mobility under the trap-free condition owing to some circumstances.

2-6 Microscopic Carrier Transport

As the activation energy ΔE of μ_f is field-independent as shown in Fig. 2-4, the Poole-Frenkel effect is not operative in μ_f . This result indicates that T_0 characteristic to the overall drift mobility is no longer defined for μ_f . The carrier transport between traps is different from the overall carrier transport. In the carrier transport process under the trap-free condition, the carriers seem to drift through the short ranged pass of the relatively ordered structure along the polymer chain without traps. There still exists, however, a small energy barrier of $\Delta E = 0.12$ eV. It was attempted to make this microscopic carrier transport process clear in terms of a phonon-assisted hopping model from molecule to molecule.

The overlap of π -electron between neighboring carbazole rings will be poor to construct a narrow band because of its

amorphous characteristics. Therefore it is much reasonable to apply a hopping model to the carrier transport under the trap-free condition in PVCz. In the simplest type of hopping transport theory [42,43] the drift mobility μ is given by

$$\mu = 2 \cdot a \cdot v_0 \cdot \left(\frac{1}{F} \cdot \sinh \frac{aeF}{2kT} \right) \cdot \exp(-\Delta E/kT) \quad (2-11)$$

where a is the hopping distance, v_0 the jumping frequency, e the electronic charge, F the applied electric field, k the Boltzmann constant, E the activation energy. For $aeF \ll kT$ Eq. (2-11) is reduced to the familiar type;

$$\mu = (e \cdot a^2 / kT) \cdot v_0 \cdot \exp(-\Delta E/kT). \quad (2-12)$$

Applying this equation to the analysis of μ_f , μ should be replaced by μ_f . As discussed above, the introduction of T_{eff} is no longer necessary in examining Eq. (2-12). The best fitting of Eq. (2-12) to the experimental data at $F = 5 \times 10^5$ V/cm shown in Fig. 2-3 gave 3.98×10^{-3} cm²/sec as the product $a^2 \cdot v_0$. Here, 0.12 eV obtained from Fig. 2-4 was used for the activation energy. In order to estimate the phonon energy, the far-infrared spectrum of PVCz was measured from 400 to 30 cm⁻¹ as shown in Fig. 2-5. If the low frequency vibrational modes of 50 cm⁻¹ and 140 cm⁻¹ are assumed for v_0 , we obtain 5.2 Å and 3.1 Å for the hopping distance, respectively. These values are very close to the shortest spatial distance (3.4 Å) between the neighboring

carbazole rings in the 3/1-helix structure of PVCz [44].

Thus, μ_f of about 10^{-3} $\text{cm}^2/\text{sec.V}$ may be considered to be the microscopic drift mobility for the carriers running through the neighboring carbazole rings until they are trapped by the usual trap sites with the depth of about 0.5 eV.

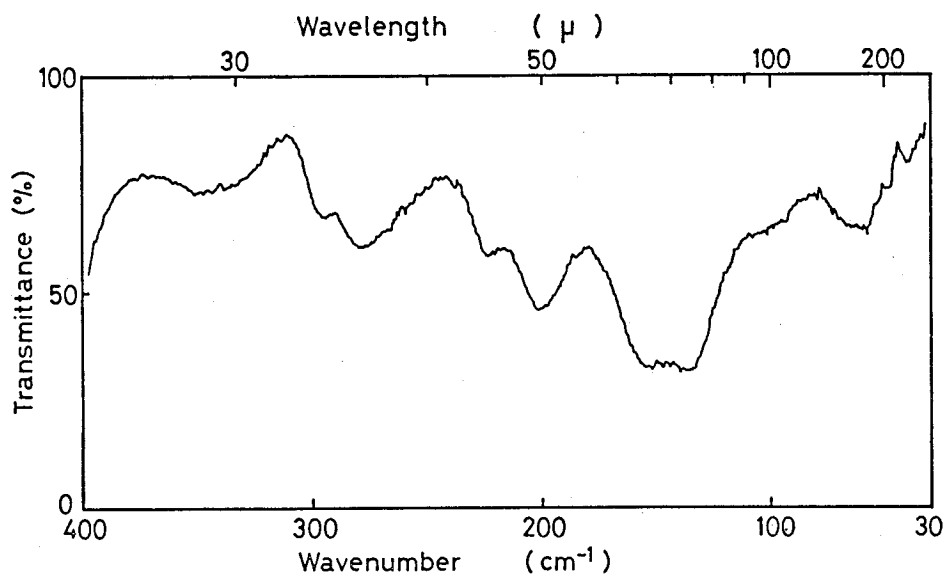


Fig. 2-5. Absorption spectrum of a PVCz film in the far-infrared region.

2-7 Conclusion

Trap-free drift mobility in PVCz was estimated directly from the current value in transient photocurrent curves by introducing a new idea of the thermal equilibrium between trapped and free carriers.

(1) The value of about $1 \times 10^{-3} \text{ cm}^2/\text{sec.V}$ was obtained for the trap-free drift mobility which is larger by about four orders than the overall drift mobility. This value seems to be an inherent upper limit of the drift mobility in amorphous polymers such as PVCz.

(2) It was found that the disorder of molecular alignments reduces the drift mobility only by two or three orders from that of single crystal state and a larger drop of the drift mobility in PVCz is caused by carrier trapping at the sites of about 0.5 eV trap depth.

(3) Microscopic carrier transport process was explained by a hopping conduction from a carbazole chromophore to the adjacent chromophore. For this transport process not so large activation energy is required even in amorphous polymers.

(4) The results obtained above would provide a possibility to find or to develop the organic amorphous material having much larger drift mobility by the artificial control of the deep level trap.

Chapter 3

Control of Carrier Trap in Amorphous Photoconductive Polymers

3-1 Introduction

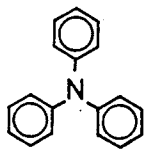
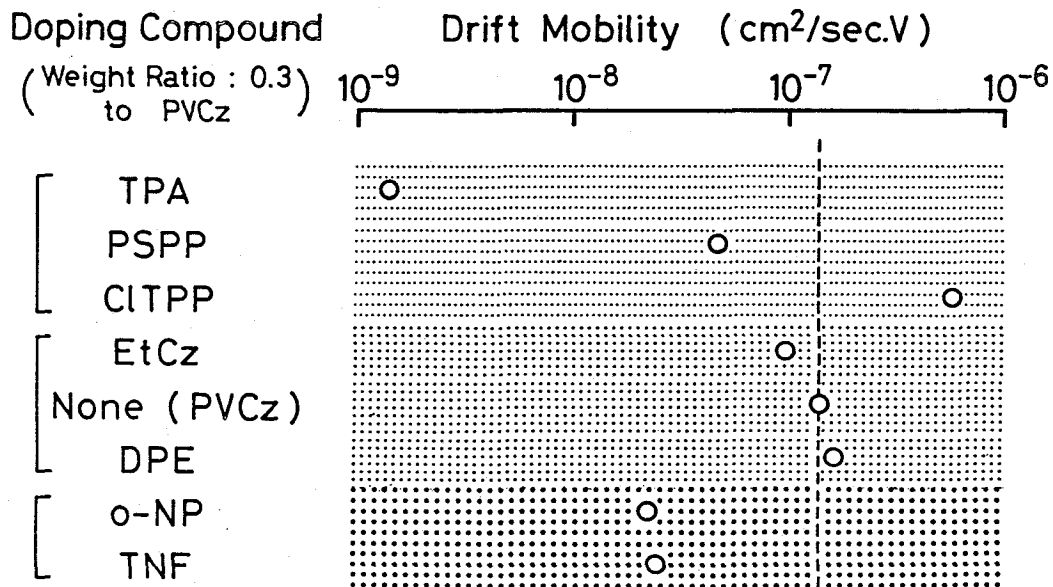
As discussed in previous chapters, the charge carrier trap in PVCz of a typical photoconductive polymer can be considered to be a structural trap, e.g., dimer site as the most plausible candidate, which can be unavoidable in amorphous usual photoconductive vinyl polymers having the π -electron system as a pendant group [45]. The essential limit of the drift mobility in PVCz was, however, estimated to be about 10^{-3} cm²/sec.V which is larger by about 4 orders in magnitude than the usually observed drift mobility of 10^{-7} cm²/sec.V. This result suggests that if we reduce the trap density in the photoconductive material, the drift mobility can be raised up to 10^{-3} cm²/sec.V. The enhancement of the drift mobility is an important problem in developing the more sensitive photoreceptors.

In this chapter, the doping effect of other compounds into PVCz was investigated. Doping of a certain low-molecular weight compound was found to give rise to the enhancement in the drift mobility of PVCz.

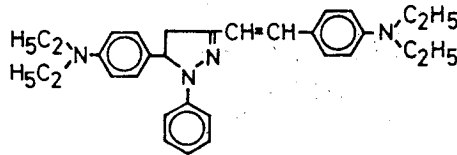
3-2 Drift Mobility in Low-molecular Weight Compound Doped PVCz System

In Fig. 3-1 are shown the drift mobilities of PVCz doped with various low-molecular weight compounds at the weight ratio of 1:0.3. Donor compounds such as triphenylamine (TPA), 1-phenyl-3-(p-diethylaminostyryl)-5-(p-diethylaminophenyl)-2-pyrazoline (PSPP) reduced the drift mobility. In the cases of donor molecules stronger than PVCz, generally, donor dopants are considered to act as a hole carrier trap, because the radical cation of donor is more stable than that of PVCz. The model compound of PVCz, EtCz or a neutral compound, 1,2-diphenylethane (DPE) reduced the drift mobility not so much as in the cases of donors. Some compounds in electron accepting group, o-nitrophenol (NP), 2,4,7-trinitrofluorenone (TNF) slightly reduced the drift mobility of PVCz. Since the ionization potential of neutral and acceptor compounds is higher than PVCz, the cation state of these compounds is not so stable as donors. These compounds will make a hopping distance among carbazole chromophores apart to reduce the drift mobility in heavy doping.

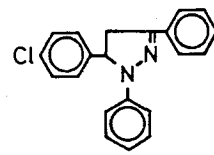
Among the various dopants used in the present study, however, one of the pyrazoline derivatives, 1,3-diphenyl-5-(p-chlorophenyl)-2-pyrazoline (ClTPP) increased the drift mobility of the system. As the ClTPP molecule is considered to be a donor to PVCz as to be discussed later, this result indicates the presence of some special interaction between PVCz



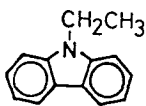
TPA



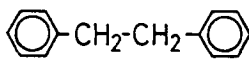
PSPP



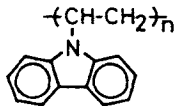
CITPP



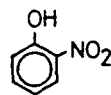
EtCz



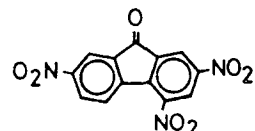
DPE



PVCz



o-NP



TNF

Fig. 3-1. Drift mobilities in various PVCz - low-molecular weight compound systems.

and ClTPP. This result suggests a possibility of improving the drift mobility with appropriate choice of dopants as a second component.

3-3 Drift Mobility in PVCz-ClTPP Binary System

The drift mobility of PVCz doped with ClTPP at room temperature is shown in Fig. 3-2 as a function of ClTPP concentration. As the concentration of ClTPP increases, the drift mobility increases and approaches the value of ClTPP glassy state in higher concentration. The value of the mobility at the weight ratio of 1:1 is about 20 times larger than that of PVCz itself. A similar observation of the enhancement in drift mobility was reported in the system of isopropylcarbazole-TPA (donor) in Lexan polymer binder [17]. In that case, the donor added in a small amount acts as a hole carrier trap as mentioned above, giving lower drift mobility. Then the drift mobility is reduced gradually at low donor concentration and beyond a critical concentration it begins to rise up to the value determined by the donor properties. In order to examine the hopping conduction from donor to donor, the drift mobility of ClTPP dispersed molecularly in polystyrene (PS) polymer binder was measured in the same range of doping concentration. This polymer binder used does not exhibit any photoconduction in the present experimental conditions. As shown in Fig. 3-2, with the increase

of ClTPP contents the drift mobility increases due to the shortening of the hopping distance among ClTPP molecules. The drift mobility in PS-ClTPP system is, however, always small by about one or more orders of magnitude when compared with that in PVCz-ClTPP system at the same content, especially, at the weight ratio of 1:0.2 the difference is about 2 orders in magnitude.

This result indicates that the increase of the drift mobility in PVCz-ClTPP system is not due to the hopping among ClTPP molecules and that the ClTPP molecules take part in hole carrier transport in this system by another kind of mechanism. Although donor compounds act as a hole carrier trap in general, it seems also possible that in some case a donor molecule promotes the carrier detrapping from the deep trap level when the trap depth due to doping donors locates between the conduction state and the deep trap level of the host compound and the dopant molecules exist in the neighborhood of the deep traps in a sufficient concentration. In what follows, we examine such a possibility in the present PVCz-ClTPP system.

In Fig. 3-3 are shown the thermally stimulated current (TSC) curves in PVCz-ClTPP (weight ratio 1:1) system. Two large peaks were observed at around $-50\text{ }^{\circ}\text{C}$ and $0\text{ }^{\circ}\text{C}$. The second peak near $0\text{ }^{\circ}\text{C}$ was observed even without the light irradiation for the carrier generation at low temperature, but not observed on the heating process after the sample was cooled down to the low temperature keeping the applied voltage. Therefore, the second

Fig. 3-2. Concentration dependence of hole drift mobility in PVCz-C1TPP and PSt-C1TPP systems.

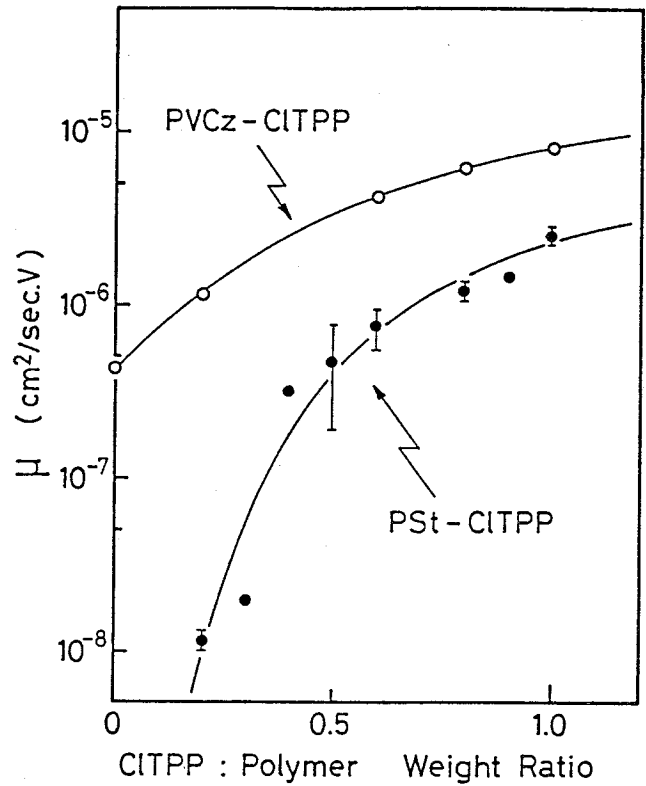
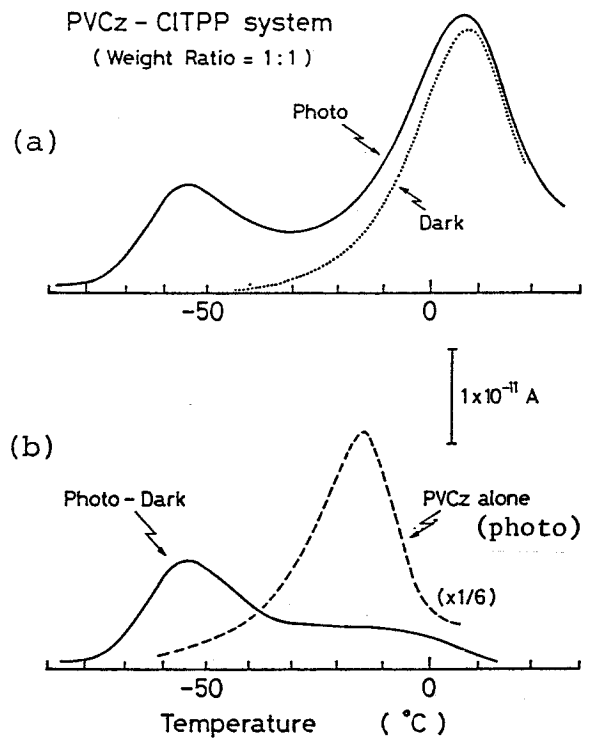


Fig. 3-3. TSC curves in PVCz-C1TPP system at 1×10^5 V/cm. Heating rate: 8 °C/min, sample thickness: 12 μm. Other experimental conditions are the same as Fig. 1-14.



peak was concluded to be due to the depolarization of ClTPP molecules. Actually, the glass transition temperature of the sample (PVCz:ClTPP = 1:1 by weight) was close to the room temperature due to the plasticizing effect as observed in the case of the PVCz-EtCz system in chapter 1. The difference of the TSC signals in the cases of with and without light irradiation is, therefore, shown in Fig. 3-3(b). In the same figure is also shown the typical TSC signal (dashed curve) of PVCz alone measured in the same experimental conditions. In the case of PVCz alone, single TSC peak was observed near -10°C with activation energy of about 0.6 eV, corresponding to the carrier detrapping from deep trap level of PVCz. However, it can be seen clearly in the differential TSC curve (solid curve) of the PVCz-ClTPP system that new peak with activation energy of about 0.4 eV appeared and that the current peak near -10°C which is characteristic to PVCz was greatly reduced. This indicates that the new shallow trap (0.4 eV) was created by doping ClTPP molecules and the detrapping event from deep trap level is considerably reduced.

In order to obtain the information about the ionization potential of PVCz and pyrazoline derivatives, the cyclic voltamograms were measured. EtCz, a model compound of PVCz was used instead of PVCz. The results are shown in Fig. 3-4. ClTPP molecule is oxidized in more negative potential by 0.35 V than EtCz molecule and PSPP molecule which acts as a hole carrier trap is oxidized more negatively by 0.8 V than EtCz. Based on

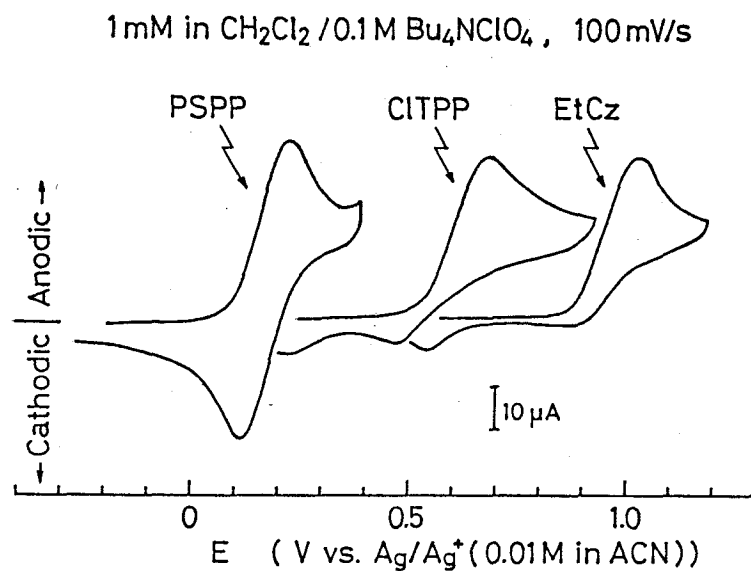


Fig. 3-4. Cyclic voltammograms of EtCz, ClTPP and PSPP at room temperature. Concentration of low-molecular weight compounds: 1 mM in CH₂Cl₂; sweep rate: 100 mV/sec.

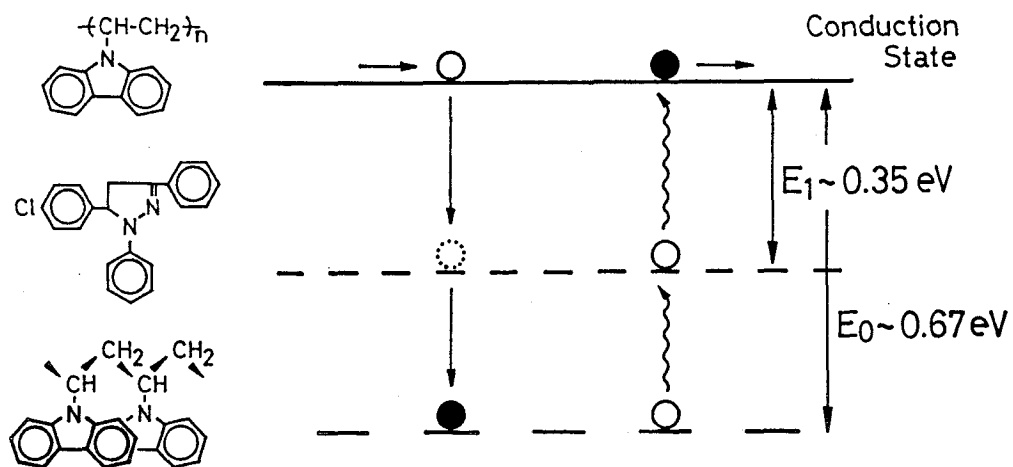


Fig. 3-5. Two-step detrapping mechanism.

the these results the energy level diagram can be drawn as shown in Fig. 3-5. The value of 0.67 eV for the deep trap of PVCz was referred from the transient photocurrent measurements. PSPP is a strong donor, and the trap level due to this compound is below the PVCz trap level. It is, therefore, reasonably understood that the doping of PSPP results in a lowering of the drift mobility. The oxidation potential of ClTPP accidentally locates between conduction state and deep trapping level to form an intermediate trapping level. If ClTPP molecules having the intermediate trapping level locate in position near the dimer trap site, the trapped carriers in deep level could be detrapped through the intermediate level with smaller activation energy than 0.6 eV, resulting in an increase of the drift mobility. Here, let us call this detrapping mechanism as 'two-step detrapping', and will be discussed in the next section.

3-4 Two-Step Detrapping Mechanism

In Fig. 3-6(a) is illustrated the trapping-detrapping events in a single deep trapping level. This case corresponds to PVCz alone. Thermally activated detrapping rate $k(0)$ under the field F is given as [43]

$$k(0) = z(0) \cdot v(0) \cdot \exp\left(-\frac{E(0) - \beta\sqrt{F}}{kT}\right). \quad (3-1)$$

Here, the Poole-Frenkel effect is taken into account, and $\nu(0)$ is the attempt-to-escape frequency, $z(0)$ the site number available for accepting a detrapped carrier, $E(0)$ trap depth from the conduction state (C.S.), respectively.

Figure 3-6(b) shows the same events in the case of two-step detrapping. Case (b) corresponds to the PVCz-ClTPP system.

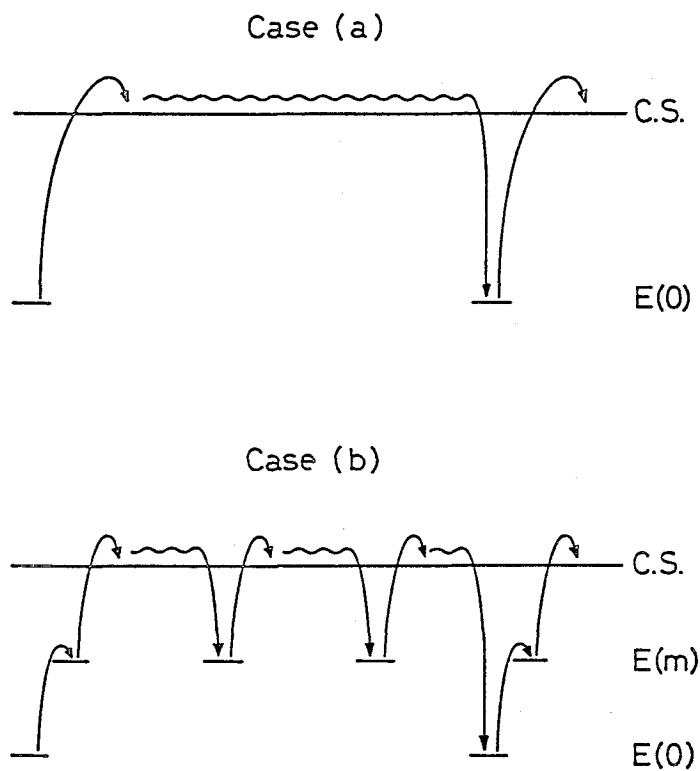


Fig. 3-6. The models of carrier detrapping mechanism. Case (a) shows the direct detrapping process and case (b) shows the two-step detrapping process. $E(0)$ and $E(m)$ denote trap depths of deep and intermediate levels from the conduction state (C.S.), respectively.

The trapped carrier in $E(0)$ level can be detrapped by two ways, i.e., direct detrapping from $E(0)$ to C.S. and two-step detrapping via intermediate trapping level $E(m)$. For the latter case, thermally activated detrapping rates, $k(1)$ for $E(0)$ to $E(m)$ and $k(2)$ for $E(m)$ to C.S., are given by the following expressions, respectively [43]:

$$k(1) = z(1) \cdot v(0) \cdot \exp\left(-\frac{E(0) - E(m)}{kT}\right) \cdot 2 \cdot \sinh\left(\frac{aeF}{2kT}\right) \quad (3-2)$$

$$k(2) = z(2) \cdot v(m) \cdot \exp\left(-\frac{E(m) - \beta\sqrt{F}}{kT}\right) \quad (3-3)$$

where $z(1)$ and $z(2)$ are the site number for each detrapping process. In hopping from $E(0)$ site to $E(m)$ site under electric field the potential barrier for the hopping event is considered to be reduced by aeF (a : hopping distance). In the second step of detrapping it is reasonable from the experiment to apply the Poole-Frenkel barrier lowering in the exponential term. Since the release time from the trap-center is defined as the inverse of the detrapping rate [45], then we obtain the following equations;

$$t_r(0) = \left[z(0) \cdot v(0) \cdot \exp\left(-\frac{E(0) - \beta\sqrt{F}}{kT}\right) \right]^{-1} \quad (3-4)$$

$$t_r(1) = \left[z(1) \cdot v(0) \cdot \exp\left(-\frac{E(0) - E(m)}{kT}\right) \cdot 2 \cdot \sinh\left(\frac{aeF}{2kT}\right) \right]^{-1} \quad (3-5)$$

$$t_r(2) = [z(2) \cdot v(m) \cdot \exp(-\frac{E(m) - \beta\sqrt{F}}{kT})]^{-1} \quad (3-6)$$

where $t_r(0)$ is the release time of detrapping from $E(0)$ to C.S., $t_r(1)$ and $t_r(2)$ are the release time for detrapplings from $E(0)$ to $E(m)$ and from $E(m)$ to C.S., respectively.

The charge carrier transport process can be described as follows.

[Case (a)] Direct detrapping from $E(0)$ to C.S.

The carriers are directly detrapped from the trap level $E(0)$ to C.S. and drift under the trap-free condition with the activation energy of about 0.1 eV as shown in Fig. 3-6(a). After a large number of hopping, s , across carbazole chromophores, the carriers are captured again by the $E(0)$ trap. This event is repeated until the carriers arrive at the counter electrode. The number, n , of these events is determined by the trap density. The transit time $t_\tau(0)$ is expressed as follows;

$$t_\tau(0) = n \cdot t_r(0) + s \cdot t(\text{free}) \quad (3-7)$$

where $t(\text{free})$ is the hopping time for each hopping event under the trap-free condition.

[Case (b)] Two-Step Detrapping via $E(m)$

The carriers are detrapped via the intermediate $E(m)$ level

and drift with the trap-free drift mobility. The carriers are also captured at the E(m) trap site. In this case, therefore, the release time from this E(m) trap should be included in evaluating the transit time. Let m be the number of detrapping events from E(m) to C.S. The number m depends on doping concentration. Thus, for the sufficient concentration of the dopant the transit time is expressed as follows;

$$\begin{aligned}
 t_{\tau}(m) &= n \cdot (t_r(1) + t_r(2)) + m \cdot t_r(2) + s \cdot t(\text{free}) \\
 &= n \cdot t_r(1) + (n + m) \cdot t_r(2) + s \cdot t(\text{free})
 \end{aligned}
 \tag{3-8}$$

The drift mobility μ is defined as

$$\mu = (d/t_{\tau})/F
 \tag{3-9}$$

(d: sample thickness, F: applied electric field)

The ratio of the drift mobility, $\mu(m)/\mu(0)$, where $\mu(0)$: the drift mobility in case (a), $\mu(m)$: the drift mobility in case (b), is calculated from the following equation:

$$\mu(m)/\mu(0) = t_{\tau}(0)/t_{\tau}(m)
 \tag{3-10}$$

Insertion of the relation of Eqs. (3-7) and (3-8) gives

$$\frac{\mu(m)}{\mu(0)} = \frac{n \cdot t_r(0) + s \cdot t(\text{free})}{n \cdot t_r(1) + (n + m) \cdot t_r(2) + s \cdot t(\text{free})} \quad (3-11)$$

Here, referring the value of about $1 \times 10^{-3} \text{ cm}^2/\text{sec.V}$ for trap-free drift mobility estimated in the previous chapter, the terms involving $t(\text{free})$ both in numerator and denominator can be negligible as compared with other terms. Thus, Eq. (3-11) can be written in a reduced form;

$$\frac{\mu(m)}{\mu(0)} = \frac{n \cdot t_r(0)}{n \cdot t_r(1) + (n + m) \cdot t_r(2)} \quad (3-12)$$

3-5 Estimation of Parameters in Eq. (3-12)

3-5-1 Estimation of n

Assuming the carrier trap in PVCz is the excimer forming site (dimer site), the value of $1-3 \times 10^{-3} \text{ mol/mol}$ unit of PVCz was reported from the excimer fluorescence measurement, which corresponds to the density of about 10^{19} cm^{-3} [33]. From this value the average distance among the dimer sites is obtained to be about 50 Å assuming three dimensional distribution. As the carriers are approved to drift along the one dimensional field direction, the hopping distance would be longer than this value.

The periodic distance of PVCz chain of 3/1-helix structure

reported to be 6.47 \AA [44]. Then the distance between the dimer sites along the main chain is $700 - 2100 \text{ \AA}$. While the trap density of $10^{16} - 10^{18} \text{ cm}^{-3}$ measured from the TSC measurement gives the value of $100 - 500 \text{ \AA}$.

Hence, we assume the value of 600 \AA for the one dimensional distance between dimer sites. This value gives $n = 1.5 \times 10^5 \text{ cm}^{-1}$.

3-5-2. Estimation of the other parameters

The number m is calculated from the following relation:

$$m = \sqrt[3]{3.7 \times 10^{21} \times (193/M) \times r} \quad (3-13)$$

where r is the molar ratio of the doped molecule, M the molecular weight of the dopant and the density of PVCz is used to be $1.2 \text{ g}\cdot\text{cm}^{-3}$.

If the 140 cm^{-1} mode of PVCz observed in the far-infrared absorption spectrum is assumed for attempt-to-escape frequency, the value of $4.2 \times 10^{12} \text{ s}^{-1}$ is obtained for $\nu(0)$. Let $\nu(m)$ be the same value as $\nu(0)$.

$z(0)$, $z(1)$ and $z(2)$ are the hopping site number available for detrapping carriers and are given as follows, respectively;

$$z(0) = \frac{1}{2} \quad (3-14)$$

$$z(1) = \frac{1}{2} \cdot \frac{r}{1+r} \quad (3-15)$$

$$z(2) = \frac{1}{2} \cdot \frac{1}{1+r} \quad (3-16)$$

where the factor 1/2 is introduced on account of the effective direction under the electric field.

Temperature T should be replaced by the effective temperature T_{eff} in amorphous polymers as mentioned in chapter 1:

$$1/T_{\text{eff}} = 1/T - 1/T_0. \quad (3-17)$$

The hopping distance 'a' from the dimer site to the ClTPP molecule is taken as the variable parameter in the calculation.

3-6 ClTPP Concentration Dependence of $\mu(m)/\mu(0)$

In evaluating the ratio of $\mu(m)/\mu(0)$ in PVCz-ClTPP system from Eq. (3-12), it was assumed that the ClTPP concentration dependence of T_0 is the same as PVCz-EtCz system obtained in chapter 1. The following values were used to calculate the ratio of $\mu(m)/\mu(0)$; $E(0) = 0.67$ eV, $E(m) = 0.35$ eV and $\beta = 3.46 \times 10^{-4} \text{ eV(V/cm)}^{-1/2}$. In Fig. 3-7 are shown the theoretical curves of $\mu(m)/\mu(0)$ with a hopping distance 'a' as a parameter. The best fit of the experimental data was obtained at $a = 11 \text{ \AA}$ which

is slightly larger than the intermolecular distance (8 \AA) of ClTPP obtained in the glassy state [20]. This value, however, seems to be acceptable for the distance between ClTPP and carbazole dimer in the amorphous polymer. Thus we have a confirmation on the 'two-step detrapping' mechanism in the present PVCz-ClTPP system.

The theoretical prediction of $\mu(m)/\mu(0)$ as a parameter of n at constant $a = 11 \text{ \AA}$ is shown in Fig. 3-8. The least deviation between the theoretical and experimental curves was obtained at $n = 1.5 \times 10^5 \text{ cm}^{-1}$, implying the pertinent estimation of trap density. A little deviation at low ClTPP concentration is considered to be due to the under estimation of T_0 or much larger chance of adjoining ClTPP in the neighborhood of the carbazole dimer site in the real system.

Activation energy of the hole drift mobility in PVCz-ClTPP (weight ratio = 1:0.3) system was obtained to be 0.33 eV at $F = 5 \times 10^5 \text{ V/cm}$ as shown in Fig. 3-9. This value is significantly smaller than 0.42 eV of PVCz itself observed at the same electric field. The value of 0.33 eV is quite close to the activation energy of the first detrapping step. Therefore, the first detrapping process would be the rate determining step, because the Poole-Frenkel effect makes the release time $t_r(2)$ from E(m) to C.S. much shorter than $t_r(1)$.

In the TSC measurement shown in Fig. 3-3(b), the relatively large peak at $-55 \text{ }^\circ\text{C}$ and the small TSC signal around at $-10 \text{ }^\circ\text{C}$ were observed. The release time in the first detrapping process at $-55 \text{ }^\circ\text{C}$ was estimated to be $1.27 \times 10^{-7} \text{ s}$ from Eq. (3-5).

Fig. 3-7. Theoretical curves of $\mu(m)/\mu(0)$ calculated from Eq. (3-12) with the hopping distance 'a' as a parameter. The closed circles show the experimental data.

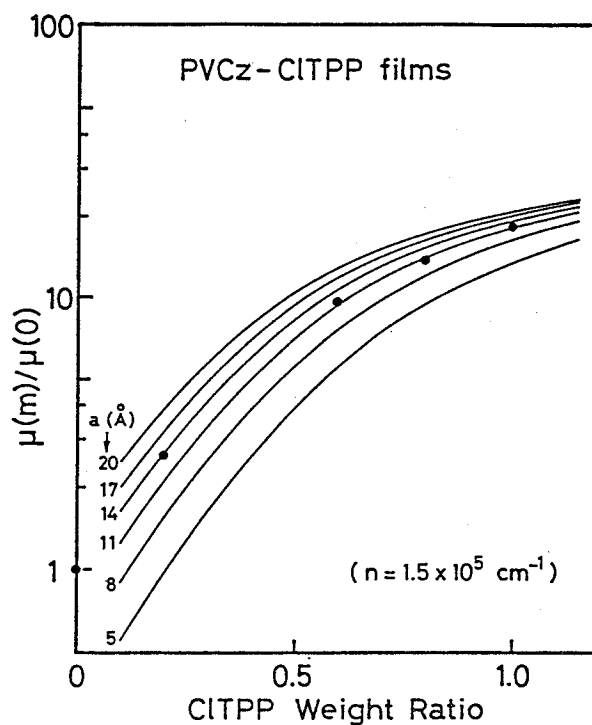
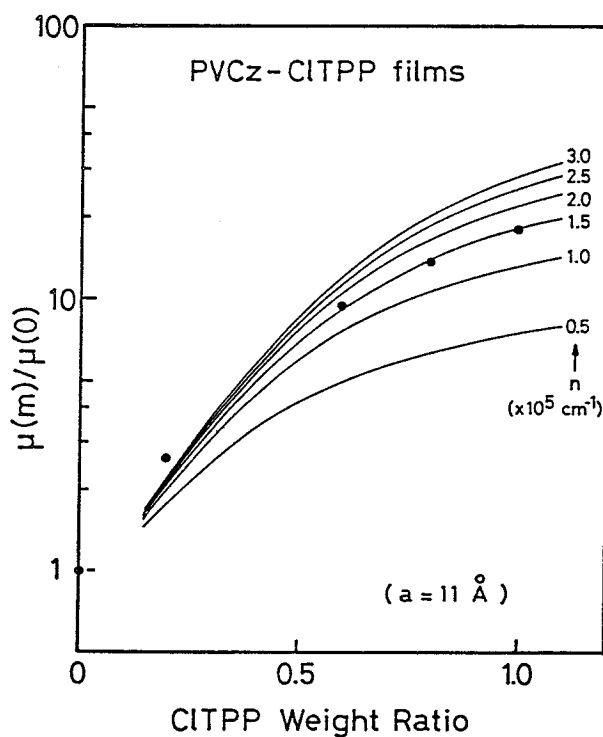


Fig. 3-8. Theoretical curves of $\mu(m)/\mu(0)$ calculated from Eq. (3-12) with the number, 'n', as a parameter. The closed circles show the experimental data.



While the release time of second step was 1.11×10^{-9} s from Eq. (3-6). Here, the effective temperature was taken into account and $a = 11 \text{ \AA}$ was assumed. The second detrapping rate is about 10^2 times faster than the first step. Therefore, the carriers detrapped from the trap level $E(0)$ to the intermediate level $E(m)$ with maximum rate at $-55 \text{ }^\circ\text{C}$ proceed immediately to the second

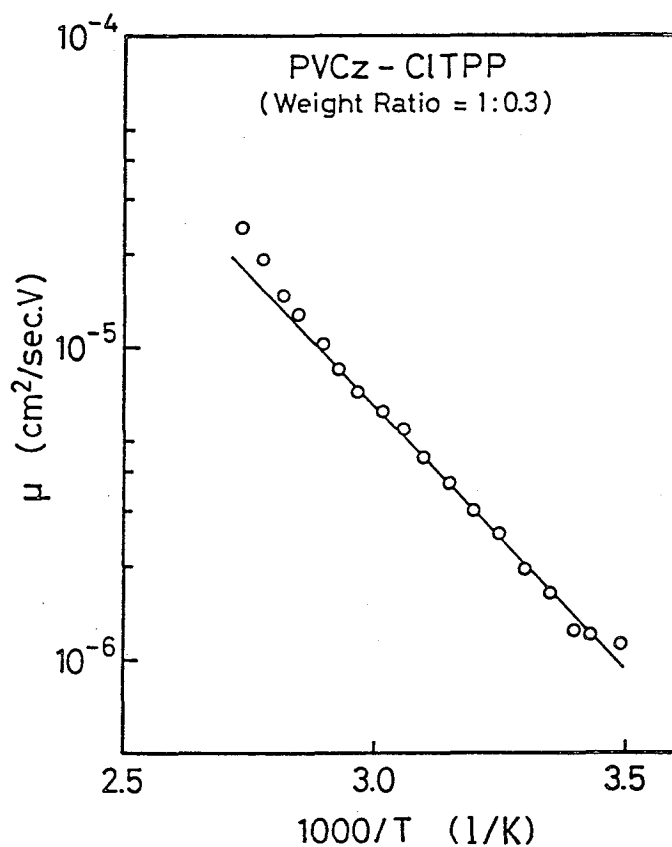


Fig. 3-9. Temperature dependence of hole drift mobility in a PVCz-CITPP (weight ratio = 1:0.3) film. The film was prepared by the bar coating method and the film thickness is $4.1 \text{ }\mu\text{m}$. The drift mobility was measured during rate heating at $1.7 \text{ }^\circ\text{C}/\text{min}$.

detrapping process from E(m) to C.S. at the same temperature. This is the reason why the TSC peak at -10°C characteristic to PVCz is reduced in the PVCz-ClTPP system.

3-7 Conclusion

In this chapter the trap control method by adding a low-molecular weight compound as the second component was investigated.

(1) Two-step detrapping mechanism was found in a two component system in which the second component provides an intermediate trap level between the conduction state level and the trap level of the host photoconductor.

(2) It was also shown that the drift mobility of amorphous polymers can be enhanced by the two-step detrapping mechanism. This result provides a new technique to improve the transport properties of the organic photoconductors.

Summary

The study in this thesis has been performed from a standpoint of understanding the charge carrier transport in amorphous photoconductive polymers. For this purpose, poly-N-vinylcarbazole (PVCz) was chosen as a research object, which had been studied so far from the wide aspects as a typical photoconductive polymer. The author believes that the following results obtained on this typical material will provide the general informations on a wide variety of other amorphous photoconductive polymers.

[1] A new experimental method was developed utilizing the plasticizing effect of the polymer by adding its low-molecular weight model compounds to find the correlation between the charge carrier transport phenomena and the thermodynamical state of the system.

[2] The critical temperature T_0 which appears in Gill's empirical expression and had been widely accepted to describe the field and temperature dependences of the drift mobility, was found to be related to the glass transition temperature of the system, at which the detrapping mechanism is changed from the field-assisted thermal detrapping to the dynamical detrapping due to the segmental motion of the polymer chain.

[3] The inherent drift mobility μ_0 at the critical temperature T_0 in Gill's empirical expression was revealed to represent the drift mobility in a supercooled liquid state of

T_0 temperature.

[4] The drift mobility of amorphous polymers was found to be described correctly by Gill's expression with the effective temperature T_{eff} based on T_0 only in the thermodynamically non-equilibrium glassy state.

[5] The essential charge carrier trap governing the transport phenomena in PVCz was shown to be a structural defect such as dimer site characteristic to amorphous vinyl polymers having a large π -electron system as a pendant group.

[6] An analytical method was developed to evaluate the trap-free drift mobility directly from the transient photocurrent value by introducing the concept of the thermal equilibrium between free and trapped carriers.

[7] A value of about $1 \times 10^{-3} \text{ cm}^2/\text{sec.V}$ was obtained as the trap-free drift mobility of PVCz, being about 10^4 times larger than the overall drift mobility of about $10^{-7} \text{ cm}^2/\text{sec.V}$.

[8] It was also found that the disorder of molecular alignments in amorphous polymers reduces the drift mobility only by two or three orders from that of single crystal state, and that the trapping process at the trap sites of about 0.5 eV in depth makes the overall drift mobility of the order of $10^{-7} \text{ cm}^2/\text{sec.V}$. This result suggested a possibility to find the organic photoconductive polymer having more effective transport properties by controlling the carrier traps characteristic to amorphous polymers.

[9] The detailed analysis of the trap-free drift mobility

in the framework of a hopping conduction model revealed that the microscopic carrier mobility is reasonably interpreted by the hopping conduction from a carbazole chromophore to the adjacent chromophore with a small activation energy of about 0.1 eV.

[10] The enhancement of the drift mobility was found in a binary system, PVCz doped with a certain low-molecular weight compound. For such an enhancement two-step detrapping mechanism was proposed. This result would give a new technique to improve the carrier transport properties of the low-mobility amorphous polymers.

References

- [1] K.R. Spangenberg, 'Fundamentals of Electron Devices', p. 408, McGraw-Hill Book Co. Inc., New York/Tronto/London (1957).
- [2] A. Pochettio, Acad. Lincei Rendicoti, 15, 355 (1906).
- [3] H. Hoegl, O. Sus and W. Neugebauer, Ger. Pat. 1068115 (1959).
- [4] P.J. Regensburger, Photochem. Photobiol., 8, 429 (1968).
- [5] W.D. Gill, J. Appl. Phys., 43, 5033 (1972).
- [6] 'Photoconductivity and Related Phenomena', ed. by J. Mort and D.M. Pai, Elsevier Publ. Co., Amsterdam/New York (1976).
- [7] A.I. Lakatos and J. Mort, Phys. Rev. Lett., 21, 1444 (1968).
- [8] J. Mort and A.I. Lakatos, J. Non-Cryst. Solids, 4, 117 (1970).
- [9] J. Mort, Phys. Rev. B, 5, 3329 (1972).
- [10] J. Mort and P. Nielsen, Phys. Rev. B, 5, 3336 (1972).
- [11] E.H. Martin and J. Hirsh, J. Non-Cryst. Solids, 4, 133 (1970).
- [12] S.M. Godson and J. Hirsh, Solid State Commun., 20, 285 (1976).
- [13] A.R. Tahmasbi and J. Hirsh, Solid State Commun., 34, 75 (1980).
- [14] P.J. Reucroft and K. Takahashi, J. Non-Cryst. Solids, 17, 71 (1975).
- [15] D.J. Williams, W.W. Limburg, J.M. Pearson, A Goedde and J.F. Yanus, J. Chem. Phys., 62, 1501 (1975).

- [16] J. Mort, G. Pfister and S. Grammatica, Solid State Commun., 18, 693 (1976).
- [17] G. Pfister, S. Grammatica and J. Mort, Phys. Rev. Lett., 37, 1360 (1976).
- [18] G. Pfister, Phys. Rev. B, 16, 3676 (1977).
- [19] G. Pfister and C.H. Griffiths, Phys. Rev. Lett., 40, 659 (1978).
- [20] H. Kitayama, M. Yokoyama and H. Mikawa, Mol. Cryst. Liq. Cryst., 69, 257 (1981); 76, 19 (1981).
- [21] H. Seki, 'Amorphous and Liquid Semiconductors', ed. by J. Stuke and W. Brenig, p. 1015, Taylor and Francis (1974).
- [22] H. Scher and E.W. Montroll, Phys. Rev. B, 12, 2455 (1975).
- [23] J.M. Marshall and A.E. Owen, Phyl. Mag., 24, 1281 (1971); Phys. Stat. Sol. (a), 12, 181 (1977); J.M. Marshall, Phyl. Mag., 36, 959 (1977); Phyl. Mag. B, 38, 335 (1978); J.M. Marshall and A.C. Sharp, J. Non-Cryst. Solids, 35 and 36, 99 (1980).
- [24] F.W. Schmidlin, Solid State Commun., 22, 451 (1977); Phys. Rev. B, 16, 2362 (1977).
- [25] M. Pollak, Phyl. Mag., 36, 1157 (1977).
- [26] J. Noolandi, Phys. Rev. B, 16, 4466 (1977); 4474 (1977).
- [27] R.J. Fleming, J. Appl. Phys., 59, 8075 (1979).
- [28] T. Demura, K. Kamisako and H. Sasabe, Polymer Preprints, Japan, 29(9), 1999 (1980).
- [29] J.H. Slowik and I. Chen, J. Appl. Phys., 54, 4467 (1983).
- [30] M. Abkowitz, M. Stolka and M. Morgan, J. Appl. Phys., 52,

3453 (1981).

- [31] T.S. Stevens and S.H. Tucker, *J. Chem. Soc.*, 123, 2140 (1923).
- [32] M. Fujino, H. Mikawa and M. Yokoyama, *J. Non-Cryst. Solids*, in press.
- [33] W. Klöpffer, *J. Chem. Phys.*, 50, 2337 (1969); K. Okamoto, A. Yano, S. Kusabayashi and H. Mikawa, *Bull. Chem. Soc. Jpn.*, 47, 749 (1974).
- [34] J.H. Sharp, *J. Phys. Chem.*, 71, 2587 (1967).
- [35] D.M. Pai, *J. Chem. Phys.*, 52, 2285 (1970); J. Patora, J. Piotrowski, K. Kryszewski and A. Szymanski, *Polym. Lett.*, 10, 23 (1972); G. Pfister and D.J. Williams, *J. Chem. Phys.*, 61, 2416 (1974); K. Kato, T. Fujimoto and H. Mikawa, *Chem. Lett.*, 63 (1975); H. Kitayama, T. Fujimoto, M. Yokoyama and H. Mikawa, 'Modification of Polymers', ed. by C.E. Carraher, Jr. and M. Tsuda, ACS Symposium Series 121., p. 205 (1980).
- [36] R.C. Hughes, *IEEE Trans. on Nuc. Sci.* NS-18, 281 (1971).
- [37] B. Reimer and H. Bässler, *Phys. Stat. Sol. (a)*, 51, 445 (1979).
- [38] J. Hirsh, *J. Phys. C: Solid St. Phys.*, 12, 321 (1979).
- [39] J. Frenkel, *Phys. Rev.*, 54, 647 (1938); R.M. Hill, *Phil. Mag.*, 23, 59 (1971).
- [40] R.C. Hughes, *Appl. Phys. Lett.*, 21, 196 (1972); *J. Chem. Phys.*, 58, 2212 (1973).
- [41] A. Szymanski and M.M. Labes, *J. Chem. Phys.*, 50, 3568 (1969).

- [42] N.F. Mott and R.N. Gurney, 'Electronic Processes in Ionic Crystals', Chap. II, Oxford, London (1948).
- [43] B.G. Bagley, Solid State Commun., 8, 345 (1970).
- [44] A. Kimura, S. Yoshimoto, Y. Akana, H. Hirata, S. Kusabayashi, H. Mikawa and N. Kasai, J. Polym. Sci., A-2, 8, 643 (1970); K. Okamoto, A. Itaya and S. Kusabayashi, J. Polym. Sci.: Polymer Physics Edition, 14, 869 (1976); C.H. Griffiths, J. Polym. Sci.: Polymer Physics Edition, 13, 1167 (1975).
- [45] C.W. Frank and L.A. Harrah, J. Chem. Phys., 61, 1526 (1974).
- [46] V.I. Arkhipov, M.S. Iovu, A.I. Rudenko and S.D. Shutov, Phys. Stat. Sol. (a), 54, 67 (1979).

List of Publications

1. Trap-Free Drift Mobility in Poly(N-vinylcarbazole).
Masaie Fujino, Hiroshi Mikawa and Masaaki Yokoyama,
Polymer Journal, 14, 81 (1982).
2. Charge Carrier Transport in Poly-N-vinylcarbazole.
Masaie Fujino, Hiroshi Mikawa and Masaaki Yokoyama,
Photographic Science and Engineering, 26, 84 (1982).
3. Charge Carrier Transport under Trap-Free Condition in PVCz.
Masaie Fujino, Hiroshi Mikawa and Masaaki Yokoyama,
Journal of Non-Crystalline Solids, in press.
4. Glass Transition in Charge Carrier Transport Phenomena of
Amorphous Photoconductive Polymers.
Masaie Fujino, Yukihiro Kanazawa, Hiroshi Mikawa,
Shigekazu Kusabayashi and Masaaki Yokoyama.
Solid State Communications, in press.
5. Enhancement of Drift Mobility of Charge Carrier in Poly(N-
vinylcarbazole)-Pyrazoline Derivative Binary System.
Masaie Fujino, Hiroshi Mikawa and Masaaki Yokoyama,
in preparation.

Acknowledgement

The author would like to express his sincerest gratitude to Professor Hiroshi Mikawa at Faculty of Engineering, Osaka University for his guidance and continuous encouragement throughout this study.

The author is deeply indebted to Associate Professor Masaaki Yokoyama, whose advice, encouragement and influence have been essential in the accomplishment of this study.

The author is also grateful to Associate Professor Yasuhiko Shirota and Dr. Takashi Nogami for their useful advices and warm encouragements.

The author makes grateful acknowledgement to Professor Shigekazu Kusabayashi for his helpful suggestions and hearty encouragement.

Thanks are also given to the author's co-worker, Mr. Yukihiro Kanazawa.

It is real pleasure to express author's thanks to all the members of the research groups of Professor Hiroshi Mikawa and Professor Shigekazu Kusabayashi for their assistance and friendships.

Finally, the author is particularly grateful to his parents, for their understanding and encouragements on this study.